

Results: Gross examination of the brain revealed a solid and hemorrhagic tumor in the pontomedullary junction. Microscopically, the tumor revealed areas of the preexisting pilocytic astrocytoma with focal transformation into a malignant lesion. Reassessment of the tumor in context of the interface with the benign lesion and the presence of classical features not seen on biopsy revealed a WHO Grade IV astrocytoma.

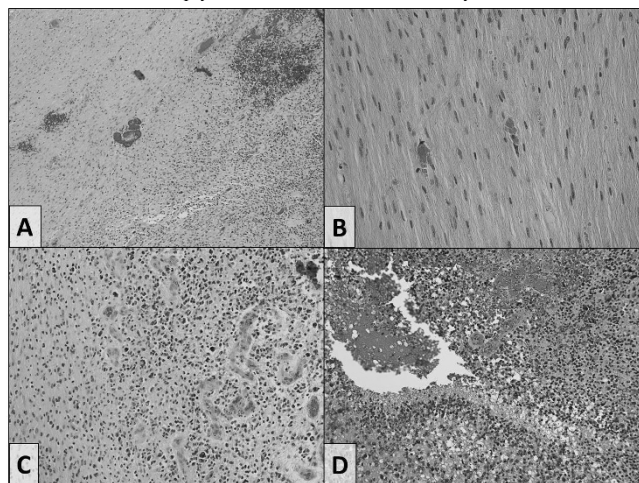


Figure 1. Low power (10x) histology reveals the interface between low- and high-grade regions of tumor (A). High power (40x) reveals a well-differentiated astrocytic neoplasm with spindle-shaped tumor cells containing elongated nuclei and abundant Rosenthal fibers (B). 20x views of the high-grade area of tumor reveal pleomorphic hypercellularity with multinucleation, nuclear lobularity and vascular endothelial proliferation (C), and pseudopalisading necrosis (D).

Molecular and immunohistochemical analysis revealed an unusual phenotype of loss of alpha thalassemia/mental retardation syndrome X-linked (ATRX) protein expression immunoreactivity, combined with wild type IDH1 and IDH2. Neither 1p nor 19q deletions were detected. Additional molecular analysis by next generation sequencing (NGS) revealed an ATM (Ataxia-telangiectasia mutated) D860N variant in both the low- and high-grade areas of the tumor.

Conclusions: Progression of NF1-associated pilocytic astrocytomas is quite rare, and the molecular features of such tumors have not been described. Recognition of unique phenotypic signatures and better understanding of the molecular events involved may lend insights into the development of high-grade astrocytomas.

30 A Novel Case of Liver-Restricted Burkitt Lymphoma in the Setting of Concomitant HBV and HCV Infections

Connor Zuraski, Katherine E Schweyte. Pathology, St Louis, MO.

Background: Primary hepatic lymphomas are rare: primary hepatic non-Hodgkin lymphomas (NHL) comprise 0.4% of all primary extranodal lymphomas and 0.016% of all non-Hodgkin's lymphomas. Diagnosis is often challenging due to the non-specific nature of the clinical signs and symptoms and difficulty distinguishing these from other primary liver malignancies. Further, up to 10% of patients are asymptomatic at the time of diagnosis. There is increasing evidence for the association of hepatitis C virus infection (HCV) and primary hepatic NHL, with diffuse large B-cell lymphoma being the most common of this group. Similarly, infection with hepatitis B virus is associated with other primary hepatic NHL, most commonly mucosa-associated lymphoid tissue (MALT) lymphoma. Primary hepatic Burkitt lymphoma is an exceedingly rare entity, with <20 cases reported in the literature, at least one of which was associated with HBV infection.

Design: We performed a search and systematic review of all autopsy reports in the electronic database of Saint Louis University Hospital from 1996-2016 using the search term 'lymphoma' (any mention in the report). The inventory of discovered cases were then organized into categories based on the number and type of organs affected by the lymphoma, concomitant neoplastic processes, association with distinct infections, and unique and potentially interesting cases.

Results: One case of primary hepatic Burkitt lymphoma was identified in a patient with a known history of HBV and HCV infections as well as cirrhosis. The patient presented with mental status changes attributed to hepatic encephalopathy. At autopsy, the liver was 2150 g and extensively nodular, including areas of central necrosis surrounded by a hemorrhagic rim. A focal area of grey-white parenchyma obscuring the cirrhotic nodules was determined to be Burkitt lymphoma by histomorphologic and immunohistochemical evaluation. Extensive evaluation revealed no other organs or lymphoid tissues to be involved by Burkitt lymphoma.

Conclusions: This appears to be the first case described in the literature of a patient co-infected with both HBV and HCV who presented at autopsy with a previously undiagnosed, primary hepatic Burkitt lymphoma. The case raises new questions about a) the role of the specific hepatitis B and C viruses, including indirect effects on immunocompetency, in the development of a non-endemic Burkitt lymphoma; b) the role of the tissue microenvironment (cirrhotic liver) in development of lymphoid malignancies in general; c) the challenging diagnosis of primary hepatic lymphoma.

Bone and Soft Tissue Pathology

31 Desmoplastic Small Round Cell Tumors (DSRCT) with Atypical Presentations: A Report of 26 Cases

Alyaa Al-Ibraheemi, Cory Broehm, Munir R Tanas, Andrew E Horvai, Brian P Rubin, Alison L Cheah, Andrew L Folpe, Karen Fritchie. Boston Childrens Hospital, Boston, MA; Mayo Clinic, Rochester, MN; University of Iowa, Iowa city, IA; UCSF, San Francisco, CA; Cleveland Clinic, Cleveland, OH; Douglass Hanly Moir, New South Wales, Australia.

Background: The overwhelming majority of DSRCTs arise in the abdominal cavity/pelvis of adolescents and young adults. Even though these tumors have a distinctive morphologic appearance, the diagnosis may be challenging when DSRCT occurs outside of this classic setting.

Design: Institutional and consultation archives were queried for cases of DSRCT presenting in patients >30 years of age or outside of the abdominal cavity/pelvis. For cases arising at an atypical location, imaging was reviewed, when available, to exclude the presence of an abdominal/pelvic mass. Only cases with 1) the presence of *EWSR1-WT1* by RT-PCR or 2) desmin/keratin immunoreactivity and the presence of *EWSR1* rearrangement by FISH were included. For cases meeting inclusion criteria, morphologic features and clinical follow-up were assessed.

Results: 26 cases were identified. Eleven (7 males, 4 females; age range 6-64 years) arose at atypical sites including neck (n=3), brain (n=3), groin (n=2), shoulder (n=1), thigh (n=1) and axilla (n=1). The remaining 15 patients were >30 years at initial presentation (13 males, 2 females; age range 32-53 years, median age 42); these tumors all involved the abdomen or pelvis. Morphologic review of the tumors showed 4 architectural patterns: micronodular (n=14), macronodular (n=5), sheet-like (n=3), and mixed (n=4). Cytomorphologic features were cataloged as: round cell (n=9), epithelioid (n=5), rhabdoid (n=5), small cell carcinoma-like (n=3), and mixed (n=4). Desmoplasia was noted in all but one case (n=25, 96%). Nine cases (36%) had punctate necrosis, and 8 cases (32%) showed geographic necrosis. The mitotic rate (per 10 high power fields) ranged from 1 to 40 (median 14). Of the 9 patients with follow-up (4 to 66 months), 7 (78%) developed metastasis, 3 (33%) were alive with disease, and 6 (67%) had died of disease.

Conclusions: DSRCT may present in patients >30 years or outside of the abdominal cavity/pelvis. Intra-abdominal tumors arising in older patients may mimic carcinoma, particularly neuroendocrine carcinoma, or rhabdomyosarcoma. It is important for pathologists to be aware that DSRCT may arise at non-abdominal locations. DSRCTs presenting in adults and at unusual sites seem to exhibit a similar male predominance and aggressive behavior as their counterparts with classic presentation.

32 Well-Differentiated Liposarcoma of the Retroperitoneum: Is There Significance to Histologic Subtyping?

Tariq Al-Zaid, Davis R Ingram, Wei-Lien Wang, Alexander J Lazar. King Faisal Specialist Hospital & Research Center, Riyadh, Saudi Arabia; The University of Texas MD Anderson Cancer Center, Houston, TX.

Background: Atypical lipomatous tumor/well differentiated liposarcoma (ALT/WDL) is a malignant mesenchymal neoplasm usually arising within the retroperitoneum, trunk or extremities of adults. There are different histologic variants including lipoma-like, sclerotic, inflammatory and cellular. We compared the clinical outcomes of the two most common subtypes--lipoma-like and sclerotic--in a series of patients with retroperitoneal WDL.

Design: The resected primary WDL tumors of 19 patients with at least three years follow-up were histologically evaluated by a soft tissue pathologist blinded to the clinical outcomes. Tumors with $\geq 25\%$ fibrosis (low-power histologic assessment) were labeled as sclerotic subtype while tumors with <25% fibrosis were labeled as lipoma-like. Cellular and inflammatory WDL tumors were not included in the study due to low prevalence.

Results: The histologic evaluation identified 5 lipoma-like WDL and 14 sclerotic WDL. The clinical follow up ranged from 3 to 11 years. At the last clinical follow up, none of patients with lipoma-like tumors died of disease (0/5; 0%) while (4/14; 28%) of sclerotic subtype patients died of disease. 25% (1/5) of lipoma-like patients were alive with disease versus 43% (6/14) of sclerotic subtype patients. 80% (4/5) of lipoma-like patients were alive without disease versus 29% (4/14) of sclerotic subtype patients.

Conclusions: In this pilot study, lipoma-like WDL of retroperitoneum showed more favorable outcome when compared with the sclerotic WDL subtype. This was evidenced by less association with death of disease and higher association with disease free survival. We are currently expanding this pilot study to include additional cases.

33 Recurrent *SRF-RELA* Fusions Define a Novel Subset of Cellular Myofibroblastic Neoplasms in the Spectrum of Cellular Myofibroma/Myopericytoma: A Potential Diagnostic Pitfall with Sarcomas with Myogenic Differentiation

Cristina R Antonescu, Yun-Shao Sung, Lei Zhang, Narasimhan P Agaram, Christopher DM Fletcher. Memorial Sloan Kettering Cancer Ctr, New York, NY; Brigham and Women's Hospital, Boston, MA.

Background: Cellular myofibroblastic tumors other than desmoid-type fibromatosis are often diagnostically challenging due to their relative rarity, lack of known genetic abnormalities, and expression of muscle markers which may be confused with sarcomas with myogenic differentiation. In this study we investigate the molecular alterations of a group of cellular myofibroblastic lesions showing morphologic overlap with the myofibroma and myopericytoma spectrum for better sub-classification.

Design: Two index cases were studied by paired-end RNA sequencing for potential fusion gene discovery. One chest wall soft tissue tumor in a 3 month-old girl case showed

a *SRF-C3orf62* fusion, while the other, a forearm lesion in an 8 year-old female, showed a *SRF-RELA* fusion. Further screening by FISH of tumors within this morphologic spectrum found an additional 6 cases with recurrent *SRF* gene rearrangements, 5 of them showing identical *SRF-RELA* fusions.

Results: The cohort was composed of 5 females and 3 males, with a wide age range of 3 months-63 years (mean 21). All tumors showed a densely packed growth of oval to spindle cells with fibrillary eosinophilic cytoplasm, arranged either in intersecting fascicles or with a distinct nested pattern around a rich vascular network. Despite the dense cellularity and variable mitotic activity none of the lesions displayed nuclear pleomorphism or necrosis. Most tumors showed reactivity for both SMA and desmin, with at least one muscle marker being diffusely positive. No myogenin staining was present. No distant metastases were seen in the few cases with follow-up information.

Conclusions: In summary we report a novel subset of cellular myofibroblastic tumors showing a smooth muscle-like immunophenotype and harboring recurrent *SRF-RELA* gene fusions, mimicking sarcomas with myogenic differentiation.

34 Synovial Sarcoma of Peripheral Nerves: Analysis of 14 Cases

John Aranake-Chrisinger, Behrang Amini, Lars-Gunnar Kindblom, Magnus Hansson, Jeanne M Meis. UT MD Anderson Cancer Center, Houston, TX; Royal Orthopaedic Hospital, Birmingham, United Kingdom; Sahlgrenska Hospital, Göteborg, Sweden.

Background: Synovial sarcoma of peripheral nerve (SSPN) is extraordinarily rare with <30 reported cases. It is often mistaken for a benign or malignant peripheral nerve sheath tumor (PNST) by pathologists, radiologists and clinicians.

Design: Cases diagnosed as SSPN were retrieved from pathology files of 3 institutions. In all cases tumor arose in a nerve by imaging, operative, gross and / or microscopic examination.

Results: 14 cases of SSPN occurring in 4 men and 10 women, 19 - 62 years old (median 39) were identified. 9 presented with neuropathic symptoms and 4 with a mass. PNST was the main clinical impression in 9 cases; another was incidentally discovered while staging a GIST. Tumor sizes were 2 - 13 cm (median 4 cm). Sites included ulnar (5), median (3), peroneal (3) and sciatic (2) nerves, and L4 nerve root (1). Treatment (known in 12 cases) was primarily surgical (12); radiation therapy (1 pre-op, 6 post-op) and chemotherapy (4) were also given. 13 tumors were monophasic and one biphasic; 3/14 had poorly differentiated (PD) areas (one rhabdoid). Hemorrhage and calcification were common (8/13 and 6/13, respectively), whereas myxoid change (4/13), necrosis (2/14), cystic change (2/13), and giant cells (2/13) were less common. Mitotic rate was low ($\leq 4/10$ hpf), except for one biphasic and 3 PD tumors (12-21/10 hpf). Expression of EMA (9/10), keratin (7/10) and TLE1 (7/7) with variable S-100 protein positivity (5/12) was noted. 11 cases were verified with molecular studies: FISH (4), RT-PCR (3) or both methods (4). Follow-up in 11 patients (2 - 122 mos, median 32) showed that 2 patients with PD tumors developed pulmonary metastases (one died) and one developed local recurrence (median 7 mos). However, 7 patients with monophasic tumors were disease free at last follow-up (median 54 mos) and one alive with disease (9 mos).

Conclusions: SSPN are likely under-recognized clinically and histologically because they closely mimic benign and malignant PNST. SSPN present unique diagnostic and therapeutic challenges by virtue of their extensive longitudinal growth within nerves, pain with poor response to drugs and risk of losing limb function with complete resection. They may have a better prognosis than comparably sized non-neural based synovial sarcomas. Molecular analysis is recommended to confirm the diagnosis. As with non-neural based tumors, poorly differentiated areas portended a worse prognosis.

35 Transducing-Like Enhancer of Split (TLE1): Promiscuous Staining Patterns in Soft Tissue and Other Neoplasms, a Diagnostic Pitfall

Samriti Arora, Anurag Sharma, Shivani Sharma, Vipin Kumar, Aurobinda Samal, Vijendra Bhandari, Arjun Singh, Santosh Pandey, Shipra Garg, Lata Kini, Sambit K Mohanty. CORE Diagnostics, Gurgaon, India.

Background: TLE1 is a relatively novel immunohistochemical (IHC) marker of synovial sarcoma (SS). However, TLE1 expression has also been observed in various soft tissue neoplasms, which raises the concern for misdiagnosis. As the specificity of TLE1 in the morphologic mimics of SS has not been extensively studied, we studied the pattern of TLE1 labeling in various soft tissue and other neoplasms and tumor-like lesions.

Design: After Institutional Review Board approval, 184 cases were included in this study and were classified as: group I: SS[40], group II: close morphologic mimics of SS (Ewing's sarcoma/primitive neuroectodermal family of tumors [25], nerve sheath tumors [15], smooth muscle neoplasms [14], rhabdomyosarcoma [6], gastrointestinal stromal tumors [5], solitary fibrous tumors [4], fibroblastic/myofibroblastic tumors [7], angiosarcoma [4], low-grade fibromyxoid sarcoma [4], dermatofibrosarcoma protuberans [3], epithelioid sarcoma [2], myositis ossificans [1], carcinomas with sarcomatoid dedifferentiation [9], and sarcomatoid mesothelioma [1]), and group III: other tumors (liposarcoma [7], pleomorphic undifferentiated sarcoma [17], inflammatory myofibroblastic tumor [1], sex-cord stromal tumor [4], hemangioperithelioma [1], malignant phyllodes tumor [1], neuroendocrine carcinoma [2], lymphoma [7], melanoma [3], and meningioma [1]). TLE1 IHC (clone 1F5) was performed and was graded as weak = 1+; moderate = 2+; strong = 3+ and 1+ (1%-25%), 2+ (26%-50%) and 3+ (51%-100%).

Results: 98%, 72%, and 61% cases of group I, II, and III, exhibited TLE1 positivity, respectively.

Tumor/Tumor Like condition	Total number of Cases	Positive Cases (%)	Intensity of Staining			Percentage of Immunoreactive cells (>50%)
			1+	2+	3+	
SYNOVIAL SARCOMA	40	39(97%)	4(10%)	4(10%)	21(50%)	7(18%)
EWING'S SARCOMA/PRIMITIVE NEUROECTODERMAL TUMOR	25	13(52%)	2(8%)	4(16%)	4(16%)	4(16%)
PLEOMORPHIC UNDIFFERENTIATED SARCOMA	17	9(53%)	3(18%)	2(12%)	4(24%)	3(18%)
PERIPHERAL NERVE SHEATH TUMOR	15	14(93%)	1(7%)	4(27%)	9(60%)	5(33%)
SMOOTH MUSCLE NEOPLASM	14	11(79%)	0(0%)	1(7%)	10(71%)	5(36%)
CARCINOMA AND CARCINOMA WITH SARCOMATOID DIFFERENTIATION	9	7(78%)	1(11%)	1(11%)	5(56%)	3(33%)
NON-HODGKIN'S LYMPHOMA	7	1(14%)	0(0%)	0(0%)	1(14%)	0(0%)
FIBROUS/MYOFIBROBLASTIC TUMOR	7	4(57%)	1(14%)	2(29%)	2(29%)	2(29%)
LIPOSARCOMA	7	7(100%)	1(14%)	2(29%)	4(57%)	2(29%)
RHABDOMYOSARCOMA	6	3(50%)	0(0%)	1(17%)	2(33%)	2(33%)
GASTROINTESTINAL STROMAL TUMOR	5	5(100%)	0(0%)	3(60%)	2(40%)	2(40%)
LOW-GRADE FIBROMYXOID SARCOMA	4	4(100%)	1(25%)	0(0%)	2(50%)	2(50%)
ANGIOSARCOMA	4	3(75%)	0(0%)	0(0%)	3(75%)	1(25%)
SEX CORD STROMAL TUMOR	4	3(75%)	1(25%)	0(0%)	2(50%)	0(0%)
SOLITARY FIBROUS TUMOR	4	3(75%)	0(0%)	0(0%)	3(75%)	3(75%)
MALIGNANT MELANOMA	3	2(67%)	0(0%)	0(0%)	2(67%)	1(33%)
DERMATOFIBROSARCOMA PROTUBERANS	3	1(33%)	1(33%)	0(0%)	0(0%)	1(33%)
EPITHELIOID SARCOMA	2	2(100%)	1(50%)	0(0%)	1(50%)	1(50%)
NEUROENDOCRINE NEOPLASM	2	2(100%)	0(0%)	1(50%)	0(0%)	2(100%)
MYOSITIS OSSIFICANS	1	1(100%)	0(0%)	1(100%)	0(0%)	1(100%)
SARCOMATOID MESOTHELIOMA	1	1(100%)	0(0%)	0(0%)	1(100%)	0(0%)
ANGIOMATOUS MENINGIOMA	1	1(100%)	0(0%)	0(0%)	1(100%)	0(0%)
INFLAMMATORY MYOFIBROBLASTIC TUMOR	1	1(100%)	0(0%)	0(0%)	1(100%)	0(0%)
MALIGNANT PHYLLODES TUMOR	1	1(100%)	0(0%)	0(0%)	1(100%)	0(0%)
HEMANGIOENDOTHELIOMA	1	0(0%)	0(0%)	0(0%)	0(0%)	0(0%)

Figure 1. Expression pattern of TLE1 in various soft tissue and other tumors and tumor like conditions.

The overall sensitivity, specificity, positive predictive value, negative predictive value, and accuracy of TLE1 for diagnosis of SS were 97.5%, 31.3%, 28.3%, 97.8%, and 45.3%, respectively, whereas with regards to the neoplasms forming its closest differential diagnoses, the specificity dropped to 28.0%.

Conclusions: TLE1 is a useful marker for SS, when used in conjunction with other immunostains and confirmed by molecular study. Promiscuity of TLE1 warrants awareness of its staining pattern in various soft tissue and other neoplasms to avoid potential diagnostic pitfalls. Further studies with a larger cohort and varieties of cases are needed to substantiate the current findings.

36 Histological Features of Giant Cell Tumor of Bone (GCTB) Following Denosumab Treatment Mimicking Well-Differentiated Osteosarcoma

Andreia Barbieri, Mukul Divatia, Rex Marco, Gerald Buchert, Jae Ro, Alberto Ayala. Houston Methodist Hospital, Houston, TX.

Background: GCTB is a locally aggressive, benign osteolytic tumor that recurs in up to 50% of patients with standard surgery based treatment. Denosumab has been recently used in the treatment of GCTB to control tumor burden in patients with large tumors, recurrence, or advanced disease. Denosumab is a fully human monoclonal antibody with specificity for RANKL, preventing its interaction with RANK, thus inhibiting the formation of osteoclastic giant cells and bone resorption. The antibody was originally introduced as a treatment of osteolytic bone disease in multiple myeloma, and bone metastases in solid tumors. Our purpose is to refine the histopathologic findings of GCTB post-treatment with Denosumab.

Design: Six patients (3 males and 3 females) with age ranging from 18 to 63 (mean 35.6) years were accrued. Tumor sites included the proximal tibia (n=1), distal radius (n=1), distal femur (n=3), and proximal femur involving the trochanter (n=1). All patients received regular cycles of Denosumab after diagnosis with advanced locally aggressive disease or after recurrence, prior to surgery.

Results: Morphologically, a prominent fibro-osseous component, foci of spindle cell proliferation and loss of osteoclast giant cells were dominant features in all cases. The fibro-osseous component dominated the picture, accounting for 60-90% of the lesion involving both the medullary cavity and extra-osseous soft tissue. It was characterized by anastomosing mature woven bony trabeculae devoid of osteoblastic activity and reminiscent of a well-differentiated osteosarcoma. The spindle cell component, accounting for up to 10-30% of the lesion, consisted of scattered foci of rounded to spindled cells with mild to moderate nuclear atypia, rare or no mitotic activity but no overt features of malignancy; it merged with the fibro-osseous component. One case exhibited areas of reactive fibrosis with scattered large nuclei. Malignant osteoid deposition was not present.

Conclusions: Denosumab-treated GCTB cases showed three main features: a dominant fibro-osseous component, cellular foci of spindle cell proliferation and absence of multinucleated giant cells; resembling well-differentiated osteosarcoma. Histologic evaluation alone, without clinical correlation, may lead to an erroneous diagnosis in such cases. Short follow-up of less than one year has shown no evidence of recurrence in this cohort. Long-term follow up will affirm the ultimate behavior of Denosumab-treated GCTB.

37 Recurrent GNAQ Mutations in Anastomosing Hemangiomas

Gregory R Bean, Nancy M Joseph, Ryan Gill, Andrew L Folpe, Andrew E Horvai, Sarah E Umetsu. University of California San Francisco, San Francisco, CA; Mayo Clinic, Rochester, MN.

Background: Anastomosing hemangiomas are recently described benign vascular lesions that occur chiefly in the genitourinary tract and paravertebral soft tissues. Owing to their rarity and cytoarchitectural features, anastomosing hemangiomas can be confused with low-grade angiosarcomas. They consist of tightly packed, capillary-sized vessels, often with fibrin thrombi, "hobnail" endothelial cells, eosinophilic globules, and extramedullary hematopoiesis. The genetic alterations underlying anastomosing hemangiomas are unknown.

Design: Cases were identified by examining excision specimens diagnosed as hemangiomas, vascular lesions, or angiosarcomas from UCSF Pathology archives.

Four cases were obtained from ALF's consultation archives. In total, 13 cases showed morphological features of anastomosing hemangioma and comprise the final study set. Capture-based next generation sequencing was performed, targeting the coding regions of ~500 cancer-related genes and select introns from ~40 genes.

Results: The clinical and sequencing data are presented below. All cases occurred in adults, and the majority were small and discovered incidentally. No cases with available clinical follow up data recurred. Nine of 13 cases (69%) showed a *GNAQ* mutation at codon 209, a known hotspot commonly mutated in uveal melanoma. No cases had any other pathogenic or likely pathogenic mutations or any detectable copy number alterations.

Case #	Location	Age/Gender	Size	Pathogenic Mutations
1	kidney/adrenal	49 M	1.2 cm	<i>GNAQ</i> p.Q209H
2	kidney	53 M	3.3 cm	<i>GNAQ</i> p.Q209L
3	adrenal	39 M	3.2 cm	<i>GNAQ</i> p.Q209H
4	peritoneum	58 M	1.7 cm	<i>GNAQ</i> p.Q209H
5	uterine myometrium	70 F	0.5 cm	<i>GNAQ</i> p.Q209H
6	periadnexal	65 F	0.5 cm	<i>GNAQ</i> p.Q209H
7	paracaval	53 M	8 cm	<i>GNAQ</i> p.Q209H
8	paravertebral	79 M	7.5 cm	<i>GNAQ</i> p.Q209H
9	spine	56 M	--	<i>GNAQ</i> p.Q209H
10	ovary	60 F	1.5 cm	--
11	spine	69 F	3.1 cm	--
12	kidney	64 M	0.7 cm	--
13	liver	66 M	1.8 cm	--

Conclusions: Identification of a recurrent *GNAQ* driver mutation provides strong evidence that anastomosing hemangiomas are indeed clonal vascular neoplasms. Moreover, as mutations in *GNAQ* have not been reported in angiosarcomas, anastomosing hemangiomas are likely distinct from malignant vascular tumors; thus testing for alterations in *GNAQ* may have diagnostic utility in difficult cases.

38 Glandular Malignant Peripheral Nerve Sheath Tumors with Neoplastic Epithelium: A Unique and Diagnostically Challenging Biphasic Neoplasm

Melissa M Blessing, Mark E Jentoft, Jorge Torres-Mora. Mayo Clinic, Rochester, MN.

Background: Glandular malignant peripheral nerve sheath tumors (MPNSTs) are rare biphasic spindle cell neoplasms with a poor prognosis, and are strongly associated with neurofibromatosis type 1 (NF1). Of the few glandular MPNSTs reported in the literature, a small subset demonstrates dysplasia to frank malignancy within the epithelial component. We report four such diagnostically challenging tumors.

Design: Institutional archives were retrospectively reviewed for MPNSTs with glandular differentiation. The initial diagnostic slides were re-reviewed by a soft tissue pathologist, neuropathologist and neuropathology fellow for distinguishing morphological features including FNCLCC grade, nature of the epithelial component, additional heterogenous components and other salient features.

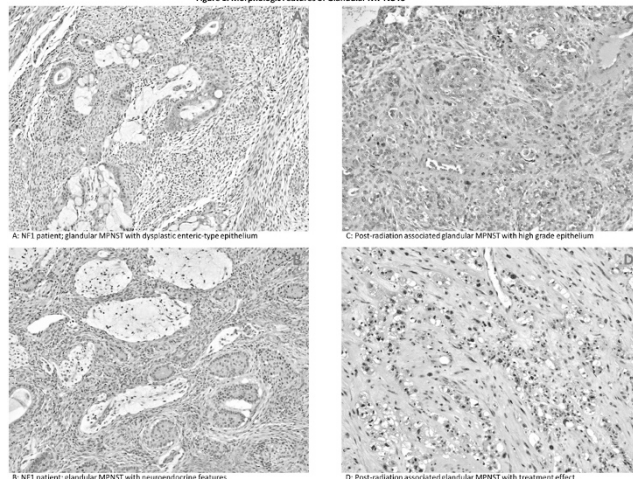
Results: Of four glandular MPNSTs, all demonstrated low to high grade neoplastic epithelium. Two patients had a NF1 history; the remaining had a history of remote radiation for other malignancies in the same region. The NF1 cases shared remarkable histologic features including enteric-type epithelium with goblet cells and mucin extravasation, as well as neuroendocrine features. The two with radiation history had less well differentiated malignant epithelium. Clinical follow-up ranged from 2-13 years; one patient with NF1 had glandular MPNST metastasis and died from their disease. The other three had no evidence of disease at last follow-up (table 1 and figure 1).

Table 1: Clinical and Pathologic Features of Four Glandular MPNSTs with Neoplastic Epithelium

Case	Clinical	Location	Initial Tumor	FNCLCC grade	Spindle component	Epithelial component	Other features
1	NF1 NED 13 years after resection & CRT	Brachial plexus	NF	3	Fibrosarcoma	Enteric-type epithelium, goblet cells, mucin extravasation; neuroendocrine; dysplastic to low grade	Solid, blastema-like islands
2	Prior thigh RT for sarcoma (>10yrs) NED 2 years after resection	Thigh	NF	2	Fibrosarcoma	Primitive high grade epithelium	Primitive neuroectodermal features
3	Prior H&N radiation (>10yrs) NED 2 years after resection	Subscapular	NF	2	Fibrosarcoma	Neuroendocrine features; goblet cell carcinoid-like and apocrine features associated with treatment effect	Extensive treatment effect from prior RT
4	NF1 Metastasis 5 years post resection; DOD	Thigh	Unknown	3	Fibrosarcoma	Enteric-type epithelium, goblet cells, mucin extravasation; neuroendocrine; dysplastic to low grade	

Key: NF = neurofibromatosis; NED = no evidence of disease; CRT = chemotherapy; RT = radiation therapy; H&N = head and neck; DOD = died of disease

Figure 1: Morphologic Features of Glandular MPNSTs



Conclusions: The morphologic features of MPNSTs with glandular differentiation are unique. While the glandular features in our NF1 cases are similar, distinguishing this neoplasm from other biphasic tumors by morphology alone is challenging, particularly in tumors secondary to radiation. However, the described findings in conjunction with the molecular features forthcoming from this institution adds diagnostic clarity and confidence.

39 Clinicopathologic Features of Giant Cell Tumor of Bone (GCT) in Patients ≥55 Years of Age: A Study of 34 Patients

Cory Broehm, Carrie Inwards, Alyaa Al-Ibraheemi, Doris Wenger, Sarah Jenkins, Long Jin, Andre Oliveira, Riyam Zreik, Jodi Carter, Jennifer M Boland, Karen Fritchie. Mayo Clinic, Rochester, MN; Baylor Scott and White Health, Temple, TX.

Background: Most GCT occur in patients aged 20 to 40 years. GCT presenting in older adults may cause diagnostic confusion with giant cell-rich lesions more common in this age group such as brown tumor of hyperparathyroidism, metastatic giant cell-rich carcinoma and sarcoma. Except for case reports and small series, the features of GCT in this age group have not been systematically studied.

Design: Primary GCT in patients ≥55 years were retrieved from our archives and examined for: fibrosis, bone/cartilage formation, cystic change, cytologic atypia, foamy histiocytes, mitotic rate/10 hpf, and necrosis. Clinical and radiologic data were reviewed. A subset was assayed for *H3F3A* mutations by PCR/sequencing.

Results: Thirty-four of 710 GCTs (4.8%) occurred in patients ≥55 years, including 14 males and 20 females (56-83 years, median 59). Sites included radius (7), tibia (6), femur (6), vertebra (6), humerus (4), pelvis (3), fibula (1) and metacarpal (1). Of tumors with available imaging, 25 of 26 cases (96%) exhibited radiologic findings classic for GCT, and all tumors arising in long bones showed epiphyseal involvement. One case had an aggressive radiologic appearance suggestive of malignancy. Morphologic patterns included: fibrosis (29 cases, 85%), bone formation (19, 56%), cystic change (8, 24%), foamy histiocytes (7, 21%) and secondary ABC (1, 3%). Mitoses ranged from 0-18 (median 5), and 8 cases (24%) harbored necrosis. No case showed cartilage or significant cytologic atypia. Follow-up data (n=33, 0-284 months, median 115) revealed 7 patients with recurrence, 1 of which developed lung metastasis. Compared to pediatric tumors, GCT in patients ≥55 years were more likely to show fibrosis (85% vs 49%, p=0.0005) and to involve the epiphysis (100% vs 79%, p=0.036). Risk of adverse events was not found to be significantly associated with necrosis (p=0.25) or mitoses (p=0.94). Four of 5 tested cases had a *H3F3A* (G34W/V) mutation.

Conclusions: GCT presenting in patients ≥55 years is rare but shares clinical, morphologic and genetic characteristics with its counterpart arising in younger patients. Interestingly, fibrosis is common in this age group, suggesting that it may be an indication of chronicity. Furthermore, mitoses and necrosis do not correlate with outcome, and pathologists should be aware of these features to avoid misclassification as malignant GCT, metastatic carcinoma or sarcoma. As nearly all tumors had a radiologic appearance classic for GCT, correlation with imaging findings will also aid in appropriate diagnosis.

40 Fusion Gene Detection in Sarcomas by the NanoString nCounter Fusion Gene Analysis Assay

Kenneth Chang, Angela Goytain, Cheng-Han Lee, Torsten Nielsen, Tony Ng. KK Women's and Children's Hospital, Singapore, Singapore; Duke-NUS Graduate Medical School, Singapore, Singapore; University of British Columbia, Vancouver, BC, Canada; Vancouver General Hospital, Vancouver, BC, Canada.

Background: Molecular characterization of sarcomas is often critical for pathological diagnosis and to direct patient management. The NanoString nCounter assay is a high-throughput hybridization technique using pooled code-sets which can assay for numerous fusion variants in a single assay. In this study, we assess the value of the NanoString assay in fusion gene detection in patient samples.

Design: We designed a customized code-set targeting 178 unique fusion junctions representing the large majority of sarcoma fusion types and variants. A few fusion types with excessive complexity at the expected junction sites (in particular *FUS-CREB3L2*) were excluded. The study cohort comprised resections and core biopsies of 133 soft tissue tumors (collected either retrospectively or prospectively), of which 48 cases had

previously demonstrated fusion genes and 85 cases had no fusions demonstrable by standard testing. RNA extracted from formalin-fixed paraffin-embedded (FFPE) tissue was hybridized with the sarcoma fusion code-set according to the nCounter protocol and analyzed with nSolver software.

Results: Of the 48 cases with confirmed fusions, our assay confirmed the result in 43 cases, including 18 of 18 Ewing sarcomas, 5 of 5 synovial sarcomas, 3 of 3 myxoid liposarcomas and 2 of 3 clear cell sarcomas. The assay was negative in 5 cases positive by FISH or RT-PCR (1 *EWSR1-ATF1*, 1 *CIC-DUX4*, 1 *WWTR-CAMTA1*, 2 *USP6* FISH-positive cases). Amongst the remaining 85 cases, fusions were discovered unexpectedly in 10 cases, including 3 *EWSR1-FLI1*/ERG cases, 2 *BCOR-CCNB3* cases, 1 *FUS-DDIT3* case and 1 *CIC-DUX4* case. There were no false positive results. In the cohort, 54 cases were collected prospectively, 18 of which were fusion positive, with no false positive or false negative results. With a batch size of 6 cases, the per sample reagent cost was \$130, total technologist time 6 hours and total turnaround time 48 hours from RNA extraction to result reporting.

Conclusions: The NanoString nCounter assay has the potential to reliably identify fusion genes in soft tissue tumors utilizing FFPE material, with rapid turnaround time and comparatively low assay cost. Based on our study results, we find the nCounter assay demonstrates sufficient sensitivity and specificity to serve as a first-line sarcoma molecular diagnostic test in a clinical setting, with next-generation sequencing-based fusion gene assays reserved for cases with unexpectedly negative results.

41 EWSR1-FLI1 Regulates PAX7 Expression in Ewing Sarcoma

Gregory Charville, Wei-Lien Wang, Jason L Hornick, Matt van de Rijn, Alexander J Lazar. Stanford University School of Medicine, Stanford, CA; The University of Texas MD Anderson Cancer Center, Boston, TX; Brigham and Women's Hospital, Boston, MA.

Background: PAX7 is a transcription factor required for the specification of adult skeletal muscle progenitors during mammalian development. Because of its role in myogenesis, we previously studied PAX7 as a marker of myogenic differentiation in rhabdomyosarcoma. Intriguingly, among a broad range of examined neoplasms, the only tumor in addition to rhabdomyosarcoma found to express PAX7 was Ewing sarcoma (ES), a malignant small round blue-cell neoplasm of bone and soft tissue which lacks a myogenic phenotype. We, therefore, sought to characterize the expression of PAX7 in a large series of ES samples and to explore the mechanism of PAX7 regulation in ES. **Design:** PAX7 protein expression was studied by immunohistochemistry in 136 ES specimens. Cases were evaluated on a tissue microarray as paired cores taken from representative areas of each FFPE block. A mouse monoclonal antibody against PAX7 was purchased from the Developmental Studies Hybridoma Bank. The antibody was used at a dilution of 1:200 (by volume) following antigen retrieval using citrate buffer. Previously deposited RNA-sequencing (RNA-seq) and ChIP-sequencing (ChIP-seq) data were accessed via Gene Expression Omnibus (Series GSE61944) and were analyzed using the Integrative Genomics Viewer.

Results: Evaluation of PAX7 antibody nuclear immunoreactivity in ES showed PAX7 expression in 93% (126/136) of specimens. Among PAX7-positive specimens, 95% (120/126) exhibited PAX7 expression in greater than 50% of tumor cell nuclei. Analysis of high-throughput sequencing data sets revealed the following observations: (1) loss of PAX7 expression upon shRNA-mediated knockdown of EWSR1-FLI1 in ES cell lines as demonstrated by RNA-seq, (2) an EWSR1-FLI1-bound candidate PAX7 enhancer in ES cell lines, (3) a peak of regulatory H3K27-acetylation at the EWSR1-FLI1-bound PAX7 enhancer in ES cell lines and primary ES, (4) loss of H3K27-acetylation at the PAX7 enhancer upon shRNA-mediated knockdown of EWSR1-FLI1, and (5) gain of H3K27-acetylation at the PAX7 enhancer in mesenchymal stem cells upon transgenic expression of EWSR1-FLI1.

Conclusions: We demonstrate PAX7 expression in a large cohort of ES cases and define a mechanism for PAX7 expression via a candidate EWSR1-FLI1-bound enhancer. Our findings suggest that analysis of PAX7 expression represents a novel tool in the approach to ES diagnosis. Future studies of PAX7 may shed light on the developmental origins and pathogenesis of ES.

42 Prognostic Value of Myogenic Differentiation in Dedifferentiated Liposarcoma

Ivan Chebib, Pawel Kurzawa, John T Mullen, Sarah E Johnstone, Vikram Deshpande, G Petur Nielsen. Massachusetts General Hospital and Harvard Medical School, Boston, MA; Poznan University of Medical Sciences, Poznan, Poland.

Background: Recently, myogenic differentiation (MD) was identified as a poor prognostic factor in retroperitoneal dedifferentiated liposarcoma (RP DDLPS). We assessed prognostic significance of: 1) MD in uniformly-treated DDLPS from a single institution, and 2) muscle mRNA expression from The Cancer Genome Atlas (TCGA) Sarcoma database.

Design: We identified a uniform single-institution cohort of RP DDLPS with standardized resection, radiochemotherapy, and follow-up. Immunohistochemical staining for MD (desmin, smooth muscle actin, calponin, caldesmon, myogenin) was performed on whole slide sections and tissue microarray. Staining was scored for strength (0: no staining; 1: weak; 2: strong) and focality (0: no staining; 1: <10% of cells; 2: 10-50%; 3: >50%). Kaplan-Meier survival analysis was assessed for overall survival (OS) and disease-free survival (DFS) at 10% positive cells and multiple other score cutoffs and significance determined by log-rank test. RP DDLPS, with MDM2 amplification, were identified in the TCGA Sarcoma database. mRNA expression of muscle-associated genes (*DES*, *ACTA1*, *ACTA2*, *ACTB*, *ACTC1*, *ACTG1*, *ACTG2*, *CALD1*, *CNN1*, *CNN2*, *MYOG*, *MYO1*, *MYF5*, *MYF6*) were evaluated by RNA-seq gene expression. Comparison of mRNA expression and overall survival status (alive/dead) or disease-free status (recurrence/disease-free) was performed by t-test.

Correlation between mRNA expression and OS or DFS was performed by Spearman rank correlation coefficient. Benjamini-Hochberg procedure was used to correct p-values for multiple hypothesis testing.

Results: 33 patients were identified with RP DDLPS. 26 cases were positive for at least 1 marker in >10% of cells. There were no statistical differences in clinicopathologic features between patients with and without MD (age, gender, tumor size, grade, completeness of resection). Evaluating 10% positivity as well as multiple other cutoffs, there was no significant association between MD and DFS ($p=0.09$) or OS ($p=0.09$). 42 patients with retroperitoneal or pelvic DDLPS with MDM2 amplification were identified in TCGA database. There was no significant survival difference between any muscle mRNA expression and overall survival status ($p=0.16$) or disease-free status ($p=0.11$). Correlation showed only weak correlation between mRNA expression and OS ($r=-0.25$, $p=0.12$) or DFS ($r=-0.38$, $p=0.10$).

Conclusions: In a uniformly treated cohort of DDLPS stained for myogenic markers and TCGA muscle mRNA expression, we found no significant correlation between MD and prognosis.

43 PD-L1 Expression in Inflammatory Myofibroblastic Tumors

Tricia R Cottrell, Christopher D Gocke, Haiying Xu, Aleksandra Ogurtsova, Janis M Taube, Deborah Belchis. Johns Hopkins University School of Medicine, Baltimore, MD.

Background: The PD-1/PD-L1 immune checkpoint pathway is important in tumor evasion of anti-tumor immunity and therapies blocking this pathway have shown efficacy in a variety of tumor types. Inflammatory myofibroblastic tumors (IMTs) are low grade malignancies often affecting children and young adults. While curable by complete resection, they often occur in a location where resection would carry morbidity. Recent studies have identified targetable ALK mutations in a subset of IMTs. However, not all tumors possess these or other targetable mutations, and in those that do, resistance is a concern. PD-L1 expression has not been explored in this tumor type.

Design: Thirty-six archival surgical pathology specimens from 28 patients ranging from 6 months to 77 years of age were included. Clinical information, including patient outcome, was obtained from the electronic record. IHC was performed for PD-L1 and CD8. ALK status was determined by IHC, FISH, or both. The percentage of cells in the immediate tumor microenvironment demonstrating membranous PD-L1 staining was scored. Tumors with >5% positive cells were considered PD-L1-positive. Intratumoral CD8 densities were assessed, and cases with ≥ 60 cells/HPF were considered CD8^{hi} (vs. CD8^{low}). The relationships between CD8 density, ALK status, and PD-L1 status were assessed.

Results: Two patients died of disease, 6 developed recurrences and were successfully treated. 18 patients were free of disease without recurrence and 2 were lost to follow up. Of the 36 tumors analyzed, 23 (62%) were positive for PD-L1. PD-L1 expression was observed on both tumor and immune cells.

	CD8 density			ALK status		
	High	Low	p-value*	+	-	p-value*
PD-L1 +	15	8	0.035	14	7	0.21
PD-L1 -	3	9		10	1	

*Fisher's exact test

Multiple specimens were available from 4 patients. In three of four cases all the tumors were concordant for PD-L1 staining; one case had 4 of 5 specimens concordant. Of the 8 tumors that recurred, all were positive for either one or both of the targetable molecules ALK and PD-L1.

Conclusions: PD-L1 expression is common in IMTs and is expressed in association with CD8 T-cells, supporting an adaptive immune resistance mechanism of tumor escape. PD-L1 expression is not associated with ALK status, suggesting that these two features should be considered independent biomarkers. Further study of the role of the PD-1/PD-L1 checkpoint pathway and potential therapeutic implications in this tumor type are warranted.

44 BRAF V600E Occurs in a Subset of Glomus Tumors, and Is Associated with Malignant Histological Characteristics

Nooshin K Dashti, Seung J Lee, Armita Bahrani, Fausto Rodriguez, Andrew L Folpe, Jennifer M Boland. Mayo Clinic, Rochester, MN; St. Jude Children's Research Hospital, Memphis, TN; Johns Hopkins Hospital, Baltimore, MD.

Background: Glomus tumors (GT) are rare mesenchymal neoplasms with a phenotype akin to the modified smooth muscle cells of the glomus body. Most are benign, but rare examples show malignant histological characteristics with associated aggressive behavior and death in up to 40% of cases. *NOTCH* rearrangements are present in 60% of GT, including benign and malignant examples. We recently encountered a malignant GT (GT-M) with *BRAF* V600E, which has been described in one small series. We sought to study a large cohort for this mutation with attention to malignant characteristics, since *BRAF* may be an attractive therapeutic target in patients with progressive disease.

Design: GT (n=102) were identified by searching our institutional and consultation archives. Diagnoses were confirmed by 2 soft tissue pathologists, and tumors were classified based on WHO criteria as benign (GT-B), uncertain malignant potential (GT-UMP; mitotic activity without nuclear atypia, OR size >2cm and deep location), or GT-M (marked nuclear atypia and mitotic activity, OR atypical mitotic figures). Clinical information was obtained from medical records and referring physicians. Cases with available material (n=94) were screened for *BRAF* V600E by immunohistochemistry. In cases with any degree of positivity, *BRAF* V600E mutation was confirmed by Sanger sequencing.

Results: The 102 GT occurred in patients aged 7-89 years (mean 49.5), without sex predilection (54% men). Most occurred in the superficial soft tissue (82%) and upper extremities (57%). The majority were GT-B (58, 57%), with 13 GT-UMP (13%) and

31 GT-M (30%). Six of 94 cases had *BRAF* V600E mutation (6.4%), including 0 of 58 GT-B, 3 of 11 GT-UMP (27%), and 3 of 25 GT-M (12%). Follow-up ≥ 6 months was obtained for 58 cases (mean 91 months, range 6-272). Three of 13 GT-M (23%) had progressive disease: 2 with metastasis at 8 and 9 years (lung, brain and heart), and 1 with enlarging residual disease at 9 months. One of 3 GT-UMP had local recurrence at 5 years (33%). One of 42 GT-B had local recurrence (2%). Follow-up of 2 GT-M and 1 GT-UMP with *BRAF* V600E showed 1 GT-M alive with disease at 9 months, and 2 without known disease at 10.75 years and 5.5 months.

Conclusions: *BRAF* V600E mutation was detected in 6.4% of GT, all of which were GT-M or GT-UMP. This mutation may be associated with a malignant phenotype in GT. In those patients with progressive disease, *BRAF* could be a promising therapeutic target.

45 **TERT Promoter Mutations in Solitary Fibrous Tumors**

Elizabeth G Demicco, Khalida Wani, Davis R Ingram, Alexander J Lazar, Wei-Lien Wang. Mount Sinai Medical Center, New York, NY; The University of Texas MD Anderson Cancer Center, Houston, TX.

Background: *TERT*, located on 5p15, encodes a protein which helps maintain chromosomal telomeres length after cell division, thus allowing continued cell proliferation and survival while cells with shortened telomeres undergo senescence and apoptosis. Recently, mutations in the telomerase reverse transcriptase (*TERT*) promoter resulting in elongated telomeres have been implicated in tumorigenesis. These mutations are a poor prognostic marker in many tumors, including sarcomas. We examined the prevalence and clinical significance of *TERT* promoter mutations in a large series of solitary fibrous tumors.

Design: DNA was extracted from FFPE tissue samples of solitary fibrous tumors (n=117). Polymerase chain reaction and Sanger sequencing was used to demonstrate the two known mutation hot spots in the *TERT* promoter (C228T and C250T). Risk assessment for aggressive disease was determined on 51 primary soft tissue tumors (low, moderate or high risk) using the published model of Demicco et al.

Results: One hundred eight samples were successfully analyzed, including 66 primary tumors (8 meningeal, 56 soft tissue and pleura), 9 local recurrences, 32 metastases, and one tumor of unknown status. Mutations in *TERT* hotspots were identified in 32 tumors (30%), the majority of which were C228T (n=29), with 3 C250T cases. Promoter mutation was associated with older age at primary diagnosis (median 60 vs 48 years, p=0.015, Mann-Whitney test), and non-meningeal origin (2/27, 7% meningeal tumors vs 30/80 38% all other sites, p=0.003). *TERT* mutations were most common in high risk tumors (8/16, 50%), were present in 7/20 (35%) moderate risk tumors, and only 3/15 (20%) low risk tumors, although this difference did not reach statistical significance (p=0.2).

Conclusions: *TERT* promoter mutations can be seen in solitary fibrous tumors and patients with tumors with this mutation might benefit from targeted telomerase inhibitor therapy. The association of *TERT* promoter mutations with older age is interesting since age is a risk factor for aggressive disease as well. Finally, mutations in the *TERT* promoter trended toward higher prevalence in primary tumors predicted to be aggressive, suggesting it could be a negative prognostic factor.

46 **Absence of Histone 3.3 Mutations in Giant Cell Tumor of Soft Tissues**

Alessandro Franchi, Alberto Righi, Marco Gambarotti, Piero Picci, Angelo P Dei Tos, Steven Billings, Lisa Simi, Irene Mancini. University of Florence, Florence, Italy; Rizzoli Institute, Bologna, Italy; Treviso Regional Hospital, Treviso, Italy; Cleveland Clinic, Cleveland, OH; University of Florence, Florence, Italy.

Background: Giant cell tumor of soft tissues (GCT-ST) is a primary soft tissue neoplasm histologically similar to GCT of bone (GCT-B). Recently, it has been reported that >90% of GCT-B have a driver mutation in the histone gene *H3F3A*, which is useful in distinction from histologic mimics. Since the relationship between GCT-ST and GCT-B is unclear, we compared a series of GCT-ST and GCT-B for the presence of *H3F3A* mutations and for immunophenotypic markers.

Design: Eight cases of GCT-ST were retrieved from our institutional archives. Fifteen GCT-B served as controls. Direct sequencing for *H3F3A* mutations in coding region between codons 1 and 42, including hot spot codons (28, 35 and 37) was performed on DNA extracted from formalin-fixed paraffin-embedded tissue. Tumors were studied immunohistochemically for RANKL, RANK, and for the osteoblastic markers SATB2 and RUNX2.

Results: None of the GCT-ST had *H3F3A* mutations, while 14 GCT-B (93.3%) were mutated (11 G35W, 1 G35V, 1 G35M and 1 G35E). All GCT-ST were positive for RANK and RUNX2, while RANKL and SATB2 were detected only in 2 cases (25%). In comparison, GCT-B showed a tendency towards higher expression of RANKL and SATB2, while RANK and RUNX2 were similarly expressed.

Conclusions: Although similar in histologic appearance and immunohistochemical profile, our results indicate that GCT-ST is distinct from GCT-B as it does not harbor *H3F3A* mutations.

47 **Fibrocartilaginous Mesenchymoma of Bone: A Clinicopathologic and Molecular Analysis of 8 Cases from a Single Institution**

Marco Gambarotti, Alberto Righi, Daniel Vanel, Stefania Cocchi, Stefania Benini, Francesca M Elli, Giovanna Mantovani, Pietro Ruggieri, Stefano Boriani, Davide M Donati, Marta Sbaraglia, Angelo P Dei Tos, Piero Picci. Rizzoli Orthopaedic Institute, Bologna, Italy; Fondazione IRCCS Ca' Granda Ospedale Maggiore Policlinico, Milan, Italy; University of Padova, Padova, Italy; Treviso Regional Hospital, Treviso, Italy.

Background: Fibrocartilaginous mesenchymoma (FM) is an extremely rare intraosseous lesion with only 25 cases are described in the literature.

Design: To better define the radiological, morphological, molecular and clinical features of FM, we retrieved from the files of the Istituto Ortopedico Rizzoli all the cases with a diagnosis of FM between 1982 and 2016.

Results: Eight cases were identified. Patient ranged in age from 8 to 27 year. Male to female ratio was 3:5. Tumors occurred in femur (2 cases), pubis (2 cases), vertebrae (2 cases), tibia (1 case), and humerus (1 case). Symptoms were pathological fracture and/or pain. At imaging the tumors appeared as poorly circumscribed lytic lesions, with cartilaginous calcifications. Cortical destructions and soft tissue invasion were present. On MRI the lesions exhibited a low signal on T1 and a high signal on T2-weighted images, with massive contrast medium uptake. Histologically, the tumors were composed of spindle cell proliferation (similar to a low-grade spindle cell sarcoma), associated with epiphyseal growth-plate-like nodules of cartilage, and bone production. The diagnosis was not performed on the initial biopsy in any of these cases due to the absence of the cartilaginous component. Molecular analysis showed absence of *GNAS* as well as of *IDH1/2* mutations. No *MDM2* amplification was found. Only one patient had a recurrence one year following intralesional resection. None died of disease.

Conclusions: FM is an extremely rare benign bone tumor with distinctive radiological and histological features, and is genetically distinct from fibrous dysplasia, low-grade osteosarcoma, and dedifferentiated chondrosarcoma. Local recurrences can be prevented with complete surgery.

48 **Distribution of Inflammatory Cells Correlates with PDL-1 Expression in Chordomas**

Sergei R Guma, Chandra Sen, Matija Snuderl. New York University Medical Center, New York, NY.

Background: Cancer immunotherapy has shown promise in recent years. The interaction of tumor programmed cell death ligand-1 (PDL-1) and programmed cell death protein (PD-1) on T cells and NK cells suppresses the cytotoxic ability of inflammatory cells, which are necessary for the immunotherapeutic effect. Several PDL-1 inhibitors have recently been approved by the FDA for a variety of cancers; however tissue biomarkers predicting the response remain to be determined for most of the tumors. We sought to elucidate the relationship between PD-L1 expression and inflammatory infiltrate in chordomas.

Design: We analyzed the expression of PDL-1 in a cohort of 15 chordomas. We evaluated intensity and distribution of the staining semi-quantitatively. We further characterized the quantity, immunophenotype and distribution of the lymphocytic inflammation involving the tumor as perivascular vs parenchymal.

Results: Thirteen (87%) chordomas were classified as conventional, 1 (6.5%) with atypical features and one (6.5%) as sarcomatoid. Eleven (73%) were clival and four (27%) were cervical. The age of the patients ranged from 18-77 years, with a mean of 45.1 years and a median of 46 years. The male: female ratio was ~1:1. PDL-1 was expressed in 87% (13/15) of the chordoma cases. 53% (8/15) of the cases had strong PDL-1 expression; 13% (2/15) had moderate PDL-1 expression and 6.7% of cases had low PDL-1 expression. Lymphocytes were a mixture of CD4+ and CD8+ cells and diffusely infiltrated the tumor parenchyma in 60% (9/15) of tumors, while in 40% (6/15) the lymphocytic infiltration was confined to the perivascular areas. PDL-1 expression was significantly stronger in tumors with tumor infiltrating lymphocytes, when compared to the tumors where inflammatory cells with perivascular inflammation (U = 8.5 by the Mann-Whitney U Test, p = 0.034). No significant correlation was found between PDL-1 expression and sex, age, tumor location, histological subtype or recurrence. No correlation was found between PDL-1 expression and clinical outcome or prognosis.

Conclusions: PDL-1 is strongly expressed in a majority of chordomas presenting PD-L1 as a potential immunotherapeutic target. The PD-L1 expression is significantly higher when the tumor's parenchyma is diffusely infiltrated by lymphocytes than when lymphocytes reside in perivascular area only, which may impact susceptibility of chordomas to PDL-1 inhibitors.

49 **PTEN Hamartoma of Soft Tissue (PHOST): A Case Series with Immunohistochemical Evaluation**

Joshua A Hanson, Lori Ballinger, Shawna Ryan, Therese Bocklage. University of New Mexico School of Medicine, Albuquerque, NM; University of New Mexico Comprehensive Cancer Center, Albuquerque, NM.

Background: PHOST is a mesenchymal lesion characterized by a disorganized proliferation of veins, thick walled arteries, and small capillaries/arterioles embedded in a fibromyxoid stroma. Its morphologic features have been described but a comprehensive immunohistochemical (IHC) analysis to examine relative proportions of vascular vs. lymphatic channels has not been performed.

Design: Five patients with a PTEN hamartoma tumor syndrome were identified. Of these, one had a resected PHOST and another had 2 resected PHOSTs. Both patients had germline PTEN mutations. IHC stains for CD34, CD31, D2-40, ERG, PROX-1, and Endoglin were performed to better characterize the abnormal vasculature within these tumors.

Results: CD34 and CD31 stained 90-100% of all vascular endothelium in each PHOSTs, though CD34 was absent in all lymphatic appearing areas. D2-40 was entirely negative

in one tumor and stained 5-10% of lymphatics in the other tumors. PROX-1 (lymphatic marker) similarly stained 5-10% of lymphatic endothelium but was positive to this degree in all tumors. ERG stained arterial and venous endothelium in all cases but did show focal (5%) lymphatic staining in one case. Endoglin demonstrated only focal positivity (5-30%) in all endothelium types and was, therefore, not discriminatory.

IHC stain	Case 1	Case 2	Case 3
CD34	100%, 3+ in arterial and venous endothelium. Absent in lymphatics.	90%, 2-3+ in arterial and venous endothelium. Absent in lymphatics.	100%, 3+ in arterial and venous endothelium. Absent in lymphatics.
CD31	100%, 3+ in all endothelium.	90%, 1+ in all arterial and venous endothelium. Absent in lymphatics.	100%, 2+ in all endothelium.
D2-40	10%, 3+ in lymphatics.	5%, 2+ in lymphatics.	Negative staining in all endothelium.
PROX-1	5%, 3+ in lymphatics.	10%, 1+ in lymphatics.	10%, 3+ in lymphatics.
ERG	50%, 3+ in arterial and venous endothelium.	95%, 3+ in all endothelium.	95%, 2-3+ in all endothelium. 5%, 2-3+ in lymphatics.
Endoglin	5%, 1-2+ in arterial and venous endothelium. Absent in lymphatics.	10%, 1+ in all endothelium.	30%, 1-2+ in all endothelium.

Conclusions: This is the first study to evaluate the proportions of vascular and lymphatic proliferations in PHOSTs using a detailed immunohistochemical analysis. Our results show only a minor component of lymphatic channels (5-10%) and thus further help define this rare hamartoma as one of primarily vascular malformations.

50 Gene Expression Profiling as a Diagnostic Adjunct for Liposarcoma

Evita Henderson-Jackson, Yin Xiong, Anthony Magliocco, Soner Altioik. Moffitt Cancer Center, Tampa, FL.

Background: Liposarcoma include five types: atypical lipomatous tumor/well-differentiated liposarcoma, dedifferentiated liposarcoma, myxoid liposarcoma, pleomorphic liposarcoma and liposarcoma (NOS). Diagnostic discordance occurs even among expert soft tissue pathologists despite advanced molecular testing. Increasing use of smaller biopsy specimens for diagnosis including overlapping histologic features, compounds the difficulty in diagnosis. We sought to develop a gene expression signature unique to liposarcoma (subtype non-specific) to serve as a diagnostic tool to distinguish liposarcoma from other sarcomas (non-liposarcomas).

Design: Retrospective study was performed on our institution's prospectively collected oncology database and all patients with a diagnosis of a soft tissue sarcoma (1993-2010) were identified. Only patients who had gene expression data were included. Differentially expressed genes for liposarcoma were compared with non-liposarcoma to identify candidate genes to create a novel gene signature specific for diagnosis of liposarcoma.

Results: 50 soft tissue sarcomas were identified with gene expression data (HuRSTA chips), 19 liposarcomas and 31 non-liposarcomas. Twenty-five significantly differentially expressed genes identified ($p < 0.01$). Principal component analysis is used to define the cutoff ($PC1 < 0 = \text{liposarcoma}$; $PC1 > 0 = \text{non-liposarcoma}$). This novel 25 gene signature is tested upon our 50 samples and 18 out of 19 liposarcomas are classified as "liposarcoma" (sensitivity=94.74%) and 29 of 31 non-liposarcomas are classified as "non-liposarcoma" (specificity=93.55%). Our 25 gene signature was tested on external data sets: (a) Paired biopsies from 6 metastatic alveolar soft part sarcoma (ASPS) classified as "non-liposarcoma" (specificity=100%) and (b) 19 Paired biopsies of untreated primary cell cultures obtained from liposarcoma {note: only 18 genes available on external chip comparable to our gene chip} classified 27 of 38 samples as "non-liposarcoma" (sensitivity=71.05%).

Conclusions: 100 samples were evaluated and 86 were correctly classified with an overall accuracy of 86%. The inappropriate classification seen with the external data set (b) could be due to only having 18 genes to compare rather than our full 25 gene signature or batch effect. Additional datasets are needed for testing; however, initial findings are promising toward the use of this gene signature as a diagnostic adjunct, especially in small biopsy specimens which would be insufficient in other molecular tests.

51 Myopericytoma: Clinicopathologic Analysis of a Series of 11 Cases with Molecular Identification of Recurrent PDGFRB Alterations

Yin (Rex) Hung, Christopher DM Fletcher. Brigham and Women's Hospital, Harvard Medical School, Boston, MA.

Background: Myopericytoma is a benign tumor characterized by concentric perivascular proliferation of myoid spindle cells. Its molecular basis and nosologic relationship with other perivascular myoid tumors, including myofibroma, myofibromatosis, and glomangiopericytoma, remain poorly understood. While it is recognized that multiple myopericytomas may develop locally in a single anatomic region, we have encountered rare cases showing diffuse dermal/subcutaneous involvement by numerous discrete myopericytoma nodules, a phenomenon we have termed myopericytomatosis.

Design: 11 cases of myopericytoma from consultation and in-house files at our institution between 1996-2016 were included. Histology and clinical information were evaluated. For molecular analysis of myopericytoma and conventional myopericytoma as comparison (5 cases each), DNA isolated from tissue sections was submitted for targeted next-generation sequencing (NGS) that interrogated exons of 300 cancer genes and selected intronic regions across 35 genes for mutations, copy number variation, and structural variants.

Results: The myopericytoma group involved 8 females and 3 males (median age 37 yr, range 9-63 yr) and often presented in the dermis/subcutis in lower extremities

(foot/ankle, 5; calf, 3; knee, 1; thigh, 1; neck, 1), over a course of several months to 25 yr, with a median size of 7.0 cm (range 1.5-11.0 cm). All showed numerous small discontinuous nodules of myopericytomatous tissue (SMA positive). All cases were treated by surgical excision (1 case with adjuvant radiation), with known margins focally positive. Of 5 cases with follow-up (median duration 2.6 yr, range 2 months to 6.5 yr), 4 showed no recurrence; one case recurred twice (at 0.5 and 1 yr) and remained disease free at 2 yr thereafter. Targeted NGS identified recurrent *PDGFRB* mutations in 4 of 5 cases of myopericytomatosis (N666K in 3 cases; in-frame deletion of Y562-R565 in 1 case) and in 3 of 5 conventional myopericytomas (K653E, Y562C, and a splice acceptor mutation in 1 case each). No mutations or copy number alterations in *BRAF* or *NOTCH* were noted.

Conclusions: Recurrent *PDGFRB* mutations are present in myopericytomatosis and conventional myopericytoma. As the activating *PDGFRB* mutation N666K, recently found in familial infantile myofibromatosis, is present in myopericytomatosis, then myopericytomatosis and myopericytoma indeed appear to lie in the same nosologic spectrum as infantile myofibromatosis and other perivascular myoid neoplasms.

52 FOSB Is a Useful Diagnostic Marker for Pseudomyogenic Hemangioendothelioma

Yin (Rex) Hung, Christopher DM Fletcher, Jason L Hornick. Brigham and Women's Hospital, Harvard Medical School, Boston, MA.

Background: Pseudomyogenic (epithelioid sarcoma-like) hemangioendothelioma (PHE) is a distinctive vascular neoplasm of intermediate biologic potential with a predilection for young adults and frequent multifocal presentation. PHE is characterized by loose fascicles of plump spindled and epithelioid cells with abundant eosinophilic cytoplasm and co-expression of keratins and endothelial markers. Recently, a *SERPINE1-FOSB* fusion has been identified as a consistent genetic alteration in PHE. *FOSB* gene fusions have also been reported in a subset of epithelioid hemangiomas. The purpose of this study was to assess the potential diagnostic utility of FOSB immunohistochemistry (IHC) for PHE compared to other endothelial neoplasms and histologic mimics.

Design: We evaluated whole-tissue sections from 274 cases including 50 PHE, 84 other vascular tumors [24 epithelioid hemangiomas (including 6 cases with angiolymphoid hyperplasia with eosinophilia histology; ALHE), 20 epithelioid angiosarcomas, 20 epithelioid hemangioendotheliomas (EHE; 17 CAMTA1-positive; 2 TFE3-positive), 10 spindle-cell angiosarcomas, and 10 epithelioid angiomatous nodules], and 140 other histologic mimics (20 each epithelioid sarcoma, proliferative fasciitis, nodular fasciitis, cellular benign fibrous histiocytoma, spindle-cell squamous cell carcinoma, spindle-cell rhabdomyosarcoma, and leiomyosarcoma). IHC for FOSB was performed following pressure cooker antigen retrieval using a rabbit monoclonal antibody (clone 5G4; Cell Signaling Technology).

Results: Diffuse nuclear immunoreactivity for FOSB (>50% of cells) was observed in 48 of 50 (96%) PHE and 13 of 24 (54%) epithelioid hemangiomas (including all ALHE-type). Both FOSB-negative PHE cases were decalcified bone tumors. Only 7 other tumors showed diffuse FOSB expression: 2 proliferative fasciitis, 2 nodular fasciitis, 1 epithelioid angiosarcoma, 1 spindle-cell angiosarcoma, and 1 EHE. Of note, the FOSB-positive EHE was negative for CAMTA1 and TFE3. All other malignant vascular neoplasms and all epithelioid sarcomas were negative for FOSB.

Conclusions: FOSB is a highly sensitive and diagnostically useful marker for PHE. IHC for FOSB may be helpful to distinguish PHE from histologic mimics including epithelioid sarcoma and other vascular neoplasms. As expected, a subset of epithelioid hemangiomas expresses FOSB, including ALHE. Although occasional cases of nodular and proliferative fasciitis are positive for FOSB, distinction between these tumor types and PHE is straightforward based on other immunophenotypic findings.

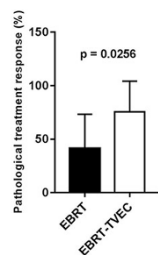
53 Tumor Response of Neoadjuvant Intralesional Injection of Talimogene Laherparepvec with Concurrent Preoperative Radiation in Patients with Locally Advanced Soft Tissue Sarcomas Compared to Neoadjuvant Radiotherapy Alone: Histopathological Assessment

Omar Jaber, Varun Monga, Mohammed Milhem, Benjamin Miller, Munir R Tanas. University of Iowa, Iowa City, IA.

Background: Talimogene laherparepvec (TVEC) is a recombinant oncolytic herpes simplex virus type 1 engineered to express GM-CSF. We hypothesized this may have an effect in sarcoma when used in combination with external beam radiation therapy (EBRT). Pathological treatment response (PTR) to immunotherapy with TVEC in combination with neoadjuvant EBRT (TVEC-EBRT) was compared to a control group receiving neoadjuvant EBRT alone.

Design: Patients with sarcomas not amenable to wide, clear margins were enrolled in the clinical trial. 9 TVEC-EBRT and 10 EBRT cases were included. The TVEC-EBRT group included undifferentiated pleomorphic sarcoma (UPS) (4), myxoid liposarcoma (ML) (2), spindle cell/ sclerosing rhabdomyosarcoma (1), myxofibrosarcoma (1) and pleomorphic liposarcoma (1). EBRT cases included UPS (4), embryonal rhabdomyosarcoma (1), dedifferentiated liposarcoma (2), ML (1), epithelioid sarcoma (1), and low grade fibromyxoid sarcoma (1). Tumor resections were evaluated post treatment. PTR including necrosis and stromal hyalinization was averaged over several blocks. Histology and immunohistochemistry for CD3, CD4, CD8, FoxP3, and CD56 were evaluated.

Results: PTR for the TVEC-EBRT group was 75.6% (mean) and 41.3% (mean) for the EBRT group ($p = 0.0256$). A lymphoplasmacytic infiltrate was identified in all TVEC-EBRT cases (9/9 cases) but only in 2 cases of EBRT (2/10) ($p = 0.0007$). EBRT cases instead demonstrated neutrophils and histiocytes. The ratio of CD8:CD4 T cells varied (1:1 to 9:1). Natural killer cells ranged from none to focal. Regulatory T cells ranged from none to 2%. No clear correlation between the composition/frequency of T cells/NK cells and PTR was identified.



Conclusions: Initial assessment of neoadjuvant immunotherapy treatment with TVEC-EBRT demonstrated a greater PTR and a lymphoplasmacytic infiltrate more frequently than EBRT alone. Additional studies are required to confirm these findings in a larger cohort of patients and identify the mechanism behind this response.

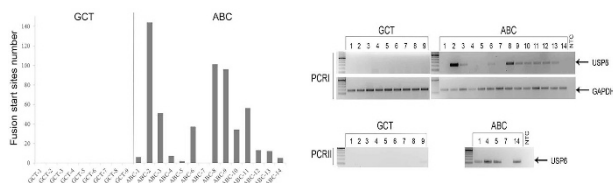
54 Upregulation of *USP6* Transcription Is Likely Driven by *USP6* Gene Fusion in Aneurysmal Bone Cyst

Omar Jaber, Natalya Guseva, Aaron A Stence, Munir R Tanas, Aaron Bossler, Deqin Ma. University of Iowa, Iowa City, IA.

Background: Primary aneurysmal bone cyst (ABC) is considered a neoplastic process due to recurrent translocations involving the *USP6* gene at the short arm of chromosome 17 (17p13). We and others have shown that *USP6* gene fusions were prevalent in primary ABC but not in giant cell tumor of the bone (GCTB). In this study, we further evaluated *USP6* gene expression in 14 cases of ABCs using a next generation sequencing (NGS)-based assay and correlated *USP6* expression levels with *USP6* gene fusions detected simultaneously by the same assay. GCTB were tested in parallel for comparison.

Design: Fourteen ABCs (13 primary and 1 secondary) and 12 GCTs were tested. Total nucleic acid was extracted from formalin-fixed, paraffin-embedded tissue. Targeted RNA sequencing for gene fusions was performed using the Universal RNA Fusion Detection Kit (ArcherDX), the Archer™ FusionPlex™ Sarcoma Panel and the Ion Torrent PGM (Life Technologies). Data were analyzed using the Archer Pipeline 3.3. The level of *USP6* expression was measured by the number of fusion start sites involving *USP6*. PCR primers flanking *USP6* coding region were used for RT-PCR and nested PCR.

Results: *USP6* RNA was detected in all 13 primary ABCs. Of which, 9 had high levels of transcripts which were confirmed by RT-PCR, and 4 had low levels of transcripts which were not detectable by a first-round of RT-PCR but were detected by a second-round nested PCR. Interestingly, the 9 cases all had *USP6* fusions identified by the pipeline. The 4 cases had very low levels of *USP6* gene fusions which could not be called confidently by the pipeline. All gene fusions resulted in fusion of the entire *USP6* coding sequence. No *USP6* fusion was detected in the case of secondary ABC or 12 cases of GCTB, and none of them had detectable *USP6* gene expression by NGS or RT-PCR followed by a second round of nested PCR.



Conclusions: Upregulation of *USP6* transcription in primary ABC was most likely driven by fusion of *USP6* coding sequence with a donor promoter. The difference in *USP6* transcript levels may be due to the different strengths of the promoters provided by the fusion partners. The prevalence of *USP6* fusion and upregulation of *USP6* expression is likely the underlying mechanism for oncogenesis in ABC.

55 *EWSR1* Fusions with CREB Family Transcription Factors Define a Novel Myxoid Mesenchymal Tumor with Predilection for Intracranial Location

Yu-Chien Kao, Yun-Shao Sung, Lei Zhang, Sumathi Vaiyapuri, Marc Rosenblum, Cristina R Antonescu. Memorial Sloan Kettering Cancer Ctr, New York, NY; Shuang Ho Hospital, Taipei Medical University, Taipei, Taiwan; The Royal Orthopaedic Hospital NHS Foundation Trust, Birmingham, United Kingdom.

Background: Recurrent gene fusions involving *EWSR1* with members of the cAMP response element binding protein (CREB) family (*ATF1* and *CREB1*) have been reported in a diverse group of tumors including angiomatoid fibrous histiocytoma (AFH), soft tissue and gastrointestinal clear cell sarcoma, primary pulmonary myxoid sarcoma and hyalinizing clear cell carcinoma of salivary gland.

Design: We have recently encountered a group of 5 myxoid mesenchymal tumors positive for *EWSR1* fusions with one of the CREB family member (*ATF1*, *CREB1* and *CREM*), with histologic features distinct from any of the previously described pathologic entities. Tumors occurred in children or young adults (12-23 years; mean 18), with equal gender distribution. All except one were intracranial (intra-axial, 2; meningeal, 2) while one was perirectal.

Results: Histologically, the tumors were well-circumscribed, often lobulated, composed of uniform ovoid to round cells, and arranged in cord-like or reticular structures in a myxoid background. All except one displayed unique sunburst amianthoid fibers. Immunohistochemically, tumors were positive for EMA (5/5; 4 focal, 1 diffuse)

and desmin (3/5). A novel *EWSR1-CREM* fusion was identified by RNA sequencing in the peri-rectal tumor, which was further confirmed by FISH and RT-PCR. A 2nd case with similar *EWSR1-CREM* fusion was identified by RT-PCR and FISH in a meningeal tumor. The remaining cases studied by FISH showed the presence of *EWSR1-CREB1* fusion in 2 cases and *EWSR1-ATF1* in one.

Conclusions: In conclusion, we report a distinct group of myxoid mesenchymal neoplasms occurring in children or young adults with a predilection for intracranial locations. Although the immunoprofile (EMA, desmin) and the fusion type raise the possibility of a myxoid AFH, none of the typical histologic findings of AFH were present, suggesting a novel entity.

56 ETV Transcriptional Upregulation Is a More Reliable Diagnostic Tool in SBRCT with *CIC* Complex Abnormalities Compared to FISH and RNAseq Methods

Yu-Chien Kao, Yun-Shao Sung, Brendan C Dickson, David Swanson, Sumathi Vaiyapuri, Shih-Chiang Huang, Cristina R Antonescu. Memorial Sloan Kettering Cancer Ctr, New York, NY; Shuang Ho Hospital, Taipei, Taiwan; Mount Sinai Hospital, Toronto, ON, Canada; Royal Orthopaedic Hospital NHS Foundation Trust, Birmingham, United Kingdom; Chang Gung Memorial Hospital, Taoyuan, Taiwan.

Background: With the advent of RNA sequencing, an increasing number of novel fusions and other genetic abnormalities have emerged recently in the spectrum of *EWSR1*-negative small blue round cell tumors (SBRCTs). *CIC* rearrangements have been reported in two-thirds of *EWSR1*-negative SBRCTs. Despite an extensive molecular work-up, a number of SBRCTs still remain unclassified.

Design: We collected 13 SBRCT cases lacking driver genetic events after RNAseq analysis using 3 different bioinformatic algorithms for fusion discovery (FusionSeq, STAR, TopHat). To further investigate the genetic alterations, RNAseq reads of *CIC* and *DUX4* genes were manually inspected. FISH for *CIC* and *DUX4* abnormalities was also performed. As SBRCTs with *CIC-DUX4* fusions show consistent up-regulation of *PEA3* transcription factors, we assessed the RNAseq expression levels of *ETV1/4/5* genes in all cases. In addition, 2 *CIC*-rearranged angiosarcomas and 12 SBRCTs with well-defined non-*CIC* genetic abnormalities were included as control group.

Results: Remarkably, all 13 cases showed high mRNA levels of *ETV1/4/5*. In the control group, only the 2 *CIC*-rearranged angiosarcomas had high *ETV1/4/5* expression, whereas all SBRCT had low levels. Upon manual inspection of the *CIC* and *DUX4* traces, 7 out of 13 cases showed low number of *CIC-DUX4* fusion reads, below the positive threshold selected in the 3 algorithms applied. Two other cases were found to have *DUX4-CIC* reads, while remaining 4 cases were negative. FISH performed in 12 cases showed *CIC* break-apart in 6 cases, including 4 lacking *CIC* abnormality on RNAseq manual inspection. However, no *CIC* abnormalities were detected by FISH in 6 cases in which the RNAseq manual inspection revealed *CIC-DUX4* or *DUX4-CIC* reads. Additional complex *CIC* intra- or extra-genic rearrangements were identified by manual detailed inspection of *CIC* gene reads in 5 cases regardless of *CIC-DUX4* fusions.

Conclusions: Our results demonstrate that FISH and RNAseq are underperforming methods in diagnosing SBRCTs with *CIC* gene abnormalities. The downstream pathway of *ETV1/4/5* transcriptional upregulation demonstrates high sensitivity and specificity in this setting and transpires as a more reliable molecular signature and diagnostic method compared to FISH and RNA sequencing.

57 BUB1B and PBK as Novel Markers in the Diagnosis of Malignant Peripheral Nerve Sheath Tumors

Meghan Kapp, Hilary Nickols, Justin MM Cates. Vanderbilt University Medical Center, Nashville, TN; Norton Brownsboro Hospital, Louisville, KY.

Background: Malignant peripheral nerve sheath tumor (MPNST) can be a challenging diagnosis with several morphologic mimics and only nonspecific immunohistochemical (IHC) markers. Recent discovery of overexpression of the mitotic regulators BUB1B and PBK in MPNST suggests that their detection may assist with diagnosis in addition to identifying possible therapeutic targets for kinase inhibitors. We therefore compared levels of BUB1B and PBK immunoreactivity in MPNST, neurofibroma, schwannoma, synovial sarcoma and fibrosarcoma.

Design: Immunohistochemistry for BUB1B and PBK was performed on a tissue microarray containing MPNST (N=13, including one transitioning from neurofibroma), neurofibroma (N=9, including 1 atypical neurofibroma), schwannoma (N=15), synovial sarcoma (N=17), and classic adult-type fibrosarcoma (N=6). Staining intensity and distribution were scored using the Allred algorithm. Statistical analysis was performed using Kruskal-Wallis and *post-hoc* Wilcoxon rank-sum tests.

Results: The median scores for BUB1B and PBK immunostains were, respectively, 4 and 0 for schwannoma, 0 and 0 for neurofibroma, 5 and 4 for MPNST, 7 and 5 for fibrosarcoma, and 6 and 4 for synovial sarcoma.

BUB1B and PBK showed significant variation in Allred scores among nerve sheath tumors (MPNST, neurofibroma, and schwannoma) (P=0.015 and P=0.046, respectively). BUB1B scores were significantly higher in MPNST compared to neurofibroma (P=0.024), but not schwannoma (P=0.71). Interestingly, the BUB1B score for the MPNST arising within a neurofibroma was 7; in contrast, the atypical neurofibroma showed a BUB1B score of 3. Subsequent *post-hoc* comparisons between different nerve sheath tumors showed no significant differences in PBK expression.

No significant differences in BUB1B or PBK IHC scores were observed among the sarcomas (MPNST, synovial sarcoma, and fibrosarcoma).

Conclusions: High BUB1B immunoreactivity in a peripheral nerve sheath tumor favors the diagnosis of MPNST over neurofibroma, but not schwannoma. It may also be informative in identifying MPNSTs transitioning from neurofibromas, but more cases need to be analyzed in this regard. BUB1B and PBK IHC does not appear helpful in differentiating MPNST from common morphologic mimics such as synovial sarcoma or fibrosarcoma.

58 Denosumab Induces the Disappearance of Osteoclastic Lineage Cells, but Failed to Eliminate the Tumor Cells of Giant Cell Tumor of Bone

Ikuma Kato, Mitsuko Furuya, Kosuke Matsuo, Reiko Tanaka, Kenichi Ohashi, Ichiro Aoki. Yokohama City University School of Medicine, Yokohama, Kanagawa, Japan; Yokohama City University Hospital, Yokohama, Kanagawa, Japan; Chiba University, Chiba, Japan.

Background: Giant cell tumor of bone (GCT) is characterized by mononuclear cells and osteoclast-like multinucleated giant cells. *H3F3A* mutation is a recently identified molecular signature of GCTs, and reported that the mutation exists only in stromal cells different from osteoclastic lineage cells. Denosumab, which is a human monoclonal antibody directed against the receptor activator of NF- κ -B ligand (RANKL), has also recently been introduced into the therapy of GCT. Although some reports said that denosumab induced tumor reduction and bone formation, it remains unclear about the tumoricidal effect. We examined the changes of histological and immunohistochemical appearance and *H3F3A* mutation status in GCTs through denosumab therapy.

Design: FFPE samples of 6 GCTs that were diagnosed in biopsy and underwent curettage after denosumab therapy were histologically reviewed and immunostained by Runx2 as an osteoblastic marker and NFATc1 as an osteoclastic marker. Nuclear staining was considered as positive. The hotspot mutation status of *H3F3A* containing a part of exon 1 was examined on FFPE samples by PCR amplification and bidirectional Sanger sequencing.

Results: All cases showed the same histological and immunohistochemical pattern. After denosumab therapy, mononuclear cells and osteoclast-like giant cells characteristic in GCT were not observed at all. Instead, mixtures of areas comprising of spindle cell proliferation or reticular woven bone formation were observed in various proportions with transitional areas. Runx2 was positive in half of the mononuclear cells before the therapy and half of the spindle cells after the therapy. NFATc1 was positive in half of the mononuclear cells and all giant cells before the therapy, but was completely negative after the therapy. All available cases before (5/5) and after (6/6) the therapy harbored *H3F3A* (G34W) mutation.

Conclusions: Denosumab therapy on GCT causes complete disappearance of osteoclastic lineage cells histologically and immunohistochemically. However, *H3F3A* mutation status suggests the tumor cells still exist. As the previous reports said, osteoclastic lineage cells do not seem to be the true tumor cells. We need more careful evaluation of the therapeutic effect of denosumab on GCT, and also need further research to identify the actual tumor cells.

59 Fibroblastic Reticular Cell Tumor (Cytokeratin-Positive Interstitial Reticulum Cell Tumor): A Series of 6 Cases with Emphasis on Extra-Nodal Presentation

Darcy A Kerr, Francisco Vega, Andrew E Rosenberg. University of Miami Miller School of Medicine, Miami, FL.

Background: Structural immune and accessory cells, also known as reticular cells, include follicular dendritic cells (FDCs), interdigitating dendritic cells (IDCs) and fibroblastic reticular cells (FRCs). Tumors of these 3 cell types are uncommon; the least is known about neoplasms of FRCs. Approximately 20 FRC tumors have been reported with the majority of cases occurring in lymph nodes; none have been reported in bone.

Design: Consultation files of one of the authors (AER) were reviewed for the diagnosis of FRC tumors. Six cases were found from 2009-2016. Clinical and demographic information was collected and available slides were reviewed.

Results: The cohort included 4 women and 2 men, 39-68 years. Two tumors occurred in bone, 1 in each posterior mediastinum, anterior mediastinal lymph node, spleen and liver. Tumor size ranged from 9-29 cm. Three tumors were well demarcated and 2 were infiltrative. The neoplastic cells were plump spindle to stellate shaped with clear to lightly eosinophilic cytoplasm arranged in short fascicles. The stroma had interspersed collagen fibers, and 2 cases showed hyalinization. Each case contained a moderately dense lymphoplasmacytic infiltrate, 1 scattered eosinophils and 1 megakaryocyte. The tumor cells had ovoid nuclei with vesicular chromatin and small to inconspicuous nucleoli; 1 case exhibited markedly irregular, lobulated nuclei and prominent red macro-nucleoli. Nuclear atypia ranged from mild (2 cases) or moderate (1) to marked (3). Two cases exhibited necrosis. Mitotic activity ranged from 0-3 mitotic figures in 10 HPF, with an atypical mitotic figure in 1 case. By immunohistochemistry, all 5 tumors tested for CK8/18 reactivity were positive. Most tumors (4/5) also demonstrated SMA positivity. All were negative for FDC markers (CD21, CD23, CD35), S100, and desmin. Clinical follow up was available for one tumor with low cytologic atypia involving the ilium, treated with curettage, cryotherapy and cement packing that recurred with a histologically similar appearance after 2 years.

Conclusions: FRC tumor is exceptionally rare and presents as a relatively large mass in a range of anatomic sites, affecting both women and men (2:1) in the 4th to 7th decades. The histology is characterized by plump spindle to stellate tumor cells with a collagenous and chronic inflammatory background. The main diagnostic differential includes FDC sarcoma, IDC sarcoma and other inflammatory pseudotumors. These correct diagnosis can usually be resolved with a panel of immunohistochemical stains.

60 Clinicopathological Prognostic Indicators of Solitary Fibrous Tumor

Jimin Kim, Yoonla Choi. Samsung Medical Center, Seoul, Republic of Korea.

Background: Solitary fibrous tumors (SFTs) are uncommon spindle-cell mesenchymal tumors, which are classified as having intermediate biological potential in the 2013 World Health Organization classification. However, SFTs present unpredictable clinical behavior. Furthermore, criteria for malignancy has not been set formally. There are few studies reporting on clinicopathological risk factors in primary solitary fibrous tumors.

Design: Institutional pathology records were reviewed to identify primary solitary fibrous tumors. Pathology slides were reviewed and scored for the presence of known histologically malignant components, including mitotic index, tumor cellularity, nuclear pleomorphism, tumor necrosis, and hemorrhage. Clinical information including patient demographics, tumor size, treatment, and outcome was obtained from medical records. Statistical analysis was performed using Kaplan-Meier analysis, Cox proportional hazards regression, and Leave-one-out validation methodology. In addition, TMA sections of formalin-fixed, paraffin-embedded tissues of SFT were stained immunohistochemically with STAT6, NAB2, CD34, P53, and Ki-67.

Results: 92 patients with resected primary solitary fibrous tumor were identified. There were no significant differences in time to local recurrence or mortality based on the site of primary solitary fibrous tumors. Tumor size (≥ 10 cm), mitotic index ($\geq 4/10$ HPFs), high tumor cellularity, high nuclear pleomorphism, and tumor necrosis predicted both time to recurrence and disease-specific mortality, respectively, except tumor hemorrhage. The predictive model in this study consisted of large tumors ≥ 10 cm, mitotic figures $\geq 4/10$ HPFs, high cellularity, high nuclear pleomorphism, and tumor necrosis had a borderline validation. Mitotic index ($\geq 4/10$ HPFs) remained predictive in both univariate and multivariate Cox model (HR=1.067, p=0.0052; HR=1.072, p=0.0129, respectively). All available SFTs (100%) showed nuclear expression of STAT6 and NAB2, which was usually diffuse and intense.

Conclusions: Large tumors ≥ 10 cm, mitotic figures $\geq 4/10$ HPFs, high cellularity, high nuclear pleomorphism, and tumor necrosis are poor prognostic indicators, especially, mitotic figures $\geq 4/10$ HPFs is a predictor of poor prognosis. Close follow-up is required for those tumors that are larger than 10cm or with the presence of histologically malignant components.

61 PD-L1 Expression in Sarcomas

Kemal Kosemehmetoglu, Ece Ozogul, Berrin Buyukeren Babaoglu, Gaye Y Gulser Tezel, Gokhan M Gedikoglu. Hacettepe University, Ankara, Turkey.

Background: Programmed death ligand 1 (PD-L1) found on tumor cells has recently been introduced to have a key role in development and dissemination of many tumors, such as lung and breast carcinomas. In this study, we retrospectively analyzed PD-L1 expression among different types of sarcomas.

Design: Tissue microarrays of 3-4 mm diameter were composed from paraffin blocks of 222 various sarcomas. Slides prepared from microarrays were stained for PD-L1 antibody (Cell Signaling, E1L3N®) using Leica Bond Autostainer. Any membranous staining over 5% of the cells was regarded as positive. Quantitative real-time PCR with TaqMan gene expression assays for PDL1 was performed using whole sections from FFPE tissue of PD-L1 positive cases, by normalizing absolute values to β -actin. Relative expression level of mRNA of PDL1 was calculated and scored using $\text{Log}_{10} \frac{2^{\text{threshold cycle of } \beta\text{-actin}}}{2^{\text{threshold cycle of PDL1}}}$.

Results: Immunohistochemically, PD-L1 expression was present in 34 of 222 (15%) sarcomas. 5/13(39%) undifferentiated pleomorphic sarcomas, 6/18(33%) malignant peripheral nerve sheath tumors, 5/16(31%), dedifferentiated liposarcomas, 4/19(21%) rhabdomyosarcomas, 2/16(13%) epithelioid sarcomas, 2/15(13%) leiomyosarcomas, 3/26(12%) synovial sarcomas, 1/18(6%) myxoid liposarcoma, 1/2(50%) extraskelatal myxoid chondrosarcoma, 1/3(33%) alveolar soft part sarcoma, 1/3(33%) parachordoma/myoepithelioma, 1/5(20%) pleomorphic liposarcoma, 1/6(14%) angiosarcoma, 1/8(13%) Ewing sarcoma showed PD-L1 expression. Cases of solitary fibrous tumor/hemangiopericytoma (18), desmoplastic round cell tumor (14), Ewing-like sarcoma (6), epithelioid hemangioendothelioma (5), clear cell sarcoma (4), myxofibrosarcoma (4), low grade fibromyxoid sarcoma (2) were all negative. Tumor infiltrating hematopoietic cells were positive for PD-L1 in 32 cases (15%) with an only 2 cases overlapping with PD-L1 staining in tumoral cells. Sixteen of 34 (47%) cases showed significant but low level PD-L1 mRNA overexpression (> 1 log).

Conclusions: We have shown PD-L1 expression in a subset of sarcomas both on protein and mRNA level. High grade pleomorphic sarcomas tend to show more frequent PD-L1 expression. Clinical trials are necessary to further assess the effect of anti PD-L1 drugs on sarcomas showing PD-L1 expression

62 Prognostic Features in Uniformly Treated Synovial Sarcoma

Ana B Larque, Vikram Deshpande, G Petur Nielsen, Ivan Chebib. Massachusetts General Hospital, Boston, MA.

Background: Synovial sarcoma (SS) is an aggressive neoplasm with few prognostic markers. The aim of the study was to: 1) identify prognostically significant clinical/pathologic features in a uniformly treated SS cohort, and 2) identify potential prognostic markers for SS from The Cancer Genome Atlas (TCGA) Sarcoma database.

Design: Cases of SS were identified that underwent uniform treatment at a single institution, including resection, radiochemotherapy and followup. Two groups were defined: 1) good behavior – patients with no evidence of disease (NED) after > 2 year followup, and 2) poor behavior – patients dead of disease (DOD) or alive with recurrence/metastasis (AWD). Clinicopathologic features were compared to identify prognostic factors differentiating the groups. To identify putative molecular prognostic markers, SS from the TCGA Sarcoma database were identified and two groups were defined: 1) living patients with > 50 months follow-up, and 2) deceased patients. Differential mRNA expression from RNA-seq gene expression was performed between these groups with the DESeq2 package for R 3.3.1.

Results: There were 121 SS (71M, 50F) with average age 41.2 years. Of these, 99 patients had followup data available: 56% showed NED, 18% DOD, and 26% AWD. The most frequent primary sites were lower-extremity (52), upper-extremity (20) and head/neck (9). Histologically, 41 cases were monophasic SS, 43 biphasic and 10 poorly differentiated (grade 3, round cell change). Comparing patients with good behavior versus poor, there was no statistically significant difference in age, sex, site, size, mono/biphasic, margin status, or necrosis. However, 9/10 poorly differentiated SS were in

the poor behavior subset ($p=.005$, Fisher exact test). There were 34 SS, not poorly differentiated, with poor behaviour but without other differentiating clinicopathologic features. Therefore, TCGA Sarcoma database was evaluated for possible prognostic markers in SS. Seven SS from TCGA Sarcoma database were identified—3 living patients and 4 deceased. Differential mRNA expression between these two groups identified 59 statistically significant genes ($q<.001$), of which a subset (eg, MET, FGF8, POSTN) play a role in carcinogenesis.

Conclusions: In review of clinicopathologic factors in a large, uniformly treated SS cohort, only poorly differentiated SS was prognostically significant. However, a subset of SS, not poorly differentiated, behaved aggressively but without other differentiating features. Analysis of SS in TCGA database identified a number of putative prognostic markers that may differentiate poor behavior in SS and require validation.

63 Upstream Regulation of Wnt Pathway in Osteosarcoma - Implications for Diagnosis and Treatment

Victor K Lee, Kenon S Chua, Huey J Lim, Cheri Chan. NUHS, Singapore, Singapore; Singapore General Hospital, Singapore, Singapore.

Background: Aberrant Wnt signaling is described in a wide range of pathological conditions both in developmental diseases and cancer. Recent studies have shown that Wnt signaling plays a critical role in normal osteoblastic and chondroblastic tissue development and bone mineralization. Aberrant Wnt Signaling has been implicated in osteosarcoma tumorigenesis. We have used a novel antibody YJ5 against Wntless (WLS), a Wnt signaling pathway protein regulating Wnt secretion, which can be used to screen different tumors for potential candidates for treatment with an upstream Wnt inhibitor drug.

Design: The objective of this study is two-fold: 1) to investigate if clinical osteosarcoma samples demonstrate aberrant Wnt signaling; as well as elevated WLS levels using YJ5 2) to investigate if osteosarcoma responds to treatment with ETC-159, a novel upstream Wnt inhibitor. Immunohistochemical expression of YJ5 was analyzed in 26 cases of osteosarcoma (both high and low grade) and 105 cases other bone tumors (benign and malignant) using a four-tiered system based on intensity (0-3+, cytoplasmic) and extent (percentage of target cells). on ETC 159, a novel PORCN inhibitor, was used to treat an osteosarcoma xenograft (SJS-1) in a murine model for 4 weeks in a two-arm randomized control study. Response to treatment was documented.

Results: 1) YJ5 was highly expressed in osteosarcoma (23 of 26 cases) and bone tumors with osteoblastic and chondroblastic differentiation (osteoblastoma, osteoid osteoma, chondroblastoma). Expression for giant cell tumors and fibrous dysplasia was variable. There was weak or absent expression in cartilaginous tumors, Ewing sarcoma and other bone tumors. 2) SJS-1 demonstrated increased tumor necrosis in the treatment arm (30-60 percent increase across all samples $p<0.005$). However, no difference in tumor volume and tumor weight was observed with treatment.

Conclusions: The YJ5 antibody is a potentially useful biomarker for identifying tumors with increased Wnt secretion that may be responsive to an upstream Wnt inhibitor. YJ5 may also be useful clinically to differentiate certain tumor types of osteoblastic origin. The use of ETC 159 for the treatment of osteosarcoma has a significant effect on tumor necrosis. Further evaluation and understanding of the mechanism of Wnt in regulating tumor pathogenesis may hold the potential for developing a curative therapeutic drug for this deadly disease.

64 Expression of MDM2 and p16 in Angiomyolipoma

Xiaoqi Lin, William B Laskin. Northwestern University, Chicago, IL.

Background: Angiomyolipoma (AML), a member of mesenchymal tumor family with perivascular epithelioid cell differentiation (PEComa), arises from the kidney. AML may grow into the retroperitoneal space mimicking a primary retroperitoneal tumor. AML is basically composed of mature adipose tissue, convoluted thick-walled blood vessels, and irregularly arranged sheets and interlacing bundles of smooth muscle. AML may be composed almost exclusively of adipocytes, which may be difficult to be distinguished from retroperitoneal well-differentiated liposarcoma. The immunomarkers, MDM2 and p16, are commonly used to make diagnosis of well-differentiated liposarcoma. In this study, we tried to test if AML expresses MDM2 and p16.

Design: A total of 17 AML cases were retrieved from our department database. Immunostains for MDM2, p16, HMB45 and melan-A were performed on sections of paraffin-embedded tissue with appropriate positive and negative controls. Staining in 10 - 50% of tumor cells was considered focal immunoreexpression and $\geq 50\%$ was categorized as diffuse.

Results: Table 1. Immunohistochemical results of AML.

Tumor	No.	Pattern	MDM2	p16	HMB45	Melan A
AML	17	Diffusely	0 (0%)	4 (24%)	7 (41%)	9 (53%)
		Focally	10 (59%)	6 (35%)	8 (47%)	7 (41%)
Total			10 (59%)	10 (59%)	15 (88%)	16 (94%)

Conclusions: Our results showed that MDM2 and p16 were focally and/or diffusely expressed in AML. Therefore, carefulness should be paid when interpreting the immunostaining results of MDM2 and p16 in a retroperitoneal mass containing adipose components, in order to avoid misinterpret AML as well-differentiated liposarcoma. Specific markers (such as HMB-45, melan A) for AML should be used to confirm the diagnoses of AML and distinguish AML from well-differentiated liposarcoma.

Our results showed that AML focally or diffuse expressed HMB45 (47% and 41%, respectively, totally 88%), and melan A (41% and 53%, respectively, tally 94%). Combination of immunostains for HMB45 and melan A will increase sensitivity for diagnosis of AML.

65 Craniofacial Osteosarcoma: A Clinicopathological Study

Chuanyong Lu, Ivana Petrovic, Lu Wang, Wen Chen, Jatin Shah, Meera Hameed. Memorial Sloan Kettering Cancer, New York, NY; Washington DC VA Medical Center, Washington, DC.

Background: Osteosarcoma of the craniofacial bones is a rare tumor. Previous studies on clinicopathological correlation are limited by either small cohorts of patients or by pooling data from the literature or multiple institutions which may have varied pathological criteria and treatment regimens. Our institution has treated 34 patients with primary craniofacial osteosarcoma during 1990 to 2016. We performed a retrospective pathological study of these cases and correlated these findings with clinical outcome.

Design: For all 34 cases, histology slides were reviewed by two pathologists, one of whom is a subspecialized bone and soft tissue pathologist. The following pathological features were noted: tumor location, tumor size, pathological subtype, tumor grade, margin status, response to neoadjuvant chemotherapy. Medical records were reviewed for neoadjuvant chemotherapy, surgery, follow-up, recurrence, and survival. Statistical analysis was performed to determine the relationship between pathological features and clinical outcomes.

Results: There were 15 females and 19 males, with ages ranging from 9 to 78 years (34+/-15 years). 16 tumors were located in maxilla, 12 in mandible, and 6 at skull base, nasothmoid complex or other locations. 26 tumors were high grade, 5 were low grade, and 3 were not graded. The predominant histological subtype of the high grade osteosarcomas were osteoblastic in 8, chondroblastic in 6, fibroblastic in 5, and were not specified in 7 cases. All patients underwent surgical resection. Thirteen patients received neoadjuvant chemotherapy. Follow up ranged from 15 to 276 months (75 +/- 62 months). Local recurrence occurred in 12 patients at 2 to 102 months after resection (28+/- 32 months). Twelve patients (35%) died at 19 to 115 months after first diagnosis (38+/- 26 months). Statistical analysis showed that tumor size ($p = 0.01$) and positive surgical margin ($p = 0.048$) had significant effect on survival. Tumor size was significantly associated with local recurrence ($p = 0.018$). Histological subtype showed marginal significance on survival ($p = 0.09$).

Conclusions: Pathological features including tumor size and margin status showed significant statistical difference on local recurrence and survival in this cohort of craniofacial osteosarcoma. Further studies on biological and molecular characteristics can shed light into the pathogenesis of these neoplasms.

66 Whole-Exome Analysis in Osteosarcoma: A Translational Research to Identify a Personalized Therapy

Massimiliano Mancini, Caterina Chiappetta, Chiara Puggioni, Vincenzo Petrozza, Chiara Mazzanti, Francesca Lessi, Paolo Aretini, Generoso Bevilacqua, Carlo Della Rocca, Claudio Di Cristofano. Sapienza University of Rome, Latina, Italy; Pisa Science Foundation, Pisa, Italy.

Background: Osteosarcoma (OS) is the most common paediatric, non hematopoietic, primary bone tumor. Although survival rate has improved considerably with neoadjuvant chemotherapy, metastatic disease still occurs in patients not responding to neoadjuvant treatment. Indeed, the survival of these young patients is related to the response to chemotherapy and eventual development of metastases. Despite many advances in cancer research, chemotherapy regimens for OS are still based on not selective cytotoxic drugs. OS is a so-called "orphan cancer" with no known driver oncogenes, for this reason finding an effective targeted therapy for the disease is a tall order. It is essential to investigate new specific molecular targeted therapies for OS to increase the overall survival of these patients.

The aim of this study was to perform exomic sequence analyses of OS to advance our understanding of their genetic underpinnings and to correlate the genetic alterations with the clinical and pathological features in each patient.

Design: The population of this study included 8 diagnostic biopsies of patients with conventional high grade OS (3 not responder to chemotherapy with metastasis; 5 responder without metastasis). Whole-exome sequencing was performed using Illumina HiSeq platform. Filtering the data by quality score, mean read depth, GMAF and using Sift and PolyPhen bioinformatics tools, we selected all variations that resulted either deleterious or probably damaging respectively.

Results: We identified 18,275 somatic variations in 8,247 genes. We found three mutated genes in 7/8 (87%) samples (KIF1B, NEB and KMT2C). KMT2C showed the highest number of variations; KMT2C is an important component of histone H3 lysine 4 methyltransferase complex and it is one of the histone modifiers previously implicated in some cancer type. Alterations of KMT2C have never been described in OS, however, this gene is implicated in regulation of the p53 gene, an oncogene frequently altered in OS.

Conclusions: Our data suggest a possible role of KMT2C in carcinogenesis, progression and resistance to therapy in osteosarcoma. We believe this integrated approach will prove useful to identify possible new strategies for early diagnosis and new therapeutic approaches and to provide a tailored treatment for each patient based on his genetic profile.

67 FISH Is a Useful Adjunct to Support Diagnostic Accuracy of Core Needle Biopsies in Soft Tissue Lesions with Suspicion of Sarcoma: Comparison Study with Open Biopsies

Arjun Mehta, William W Tseng, Michael Pepper, Shefali Chopra. Keck Medical Center of USC, Los Angeles, CA.

Background: While core needle biopsies are being increasingly used for first time diagnosis in soft tissue lesions, some still believe that open biopsy is necessary for accurate histological classification and grade of these lesions. Most of the prior studies done were before the frequent use of fluorescence in situ hybridization (FISH) as an ancillary diagnostic test. Many sarcomas have chromosomal translocations which can be detected by specific FISH tests.

Design: Clinicopathologic data for core needle, open biopsies and subsequent resection specimens for soft tissue lesions clinically suspicious for sarcoma were reviewed for a consecutive period of 20 months from February 2015 to September 2016 at our institution. The diagnoses from biopsies were compared with the final diagnosis on resection. The size, number of cores obtained and ancillary studies performed were noted.

Results: Thirty five core needle and 33 open biopsies were done during the study period. Nineteen of the core needle biopsies and 22 of the open biopsies have had subsequent resections to date. All of the core needle samples were multiple, with a thickness of 16-18 g and average of 4 cores. FISH was done in 21 of the 35 (58%) core biopsies and 14 of the 33 (42%) of open biopsies. Out of the 35 needle core biopsies 23 (58%) were sarcomas and 12 (42%) were benign. Data is summarized in table 1.

Tumor classification	CORE NEEDLE BIOPSIES				OPEN BIOPSIES				
	No. of cases	No. of malignant cases	No. of cases with FISH	No. of matched cases with resections	No. of malignant cases with FISH	No. of malignant cases	No. of cases with FISH	No. of matched cases with resections	No. of malignant cases with FISH
Fatty tumors (40%)	14	12	12	10 (53%)	11 (79%)	8 (24%)	4 (15%)	7 (50%)	5 (38%)
Round cell tumors (7%)	2	2 (9%)	2 (10%)	0 (0%)	1 (50%)	6 (18%)	6 (23%)	5 (23%)	4 (67%)
Vascular tumors (8%)	3	1 (5%)	1 (5%)	1 (5%)	0 (0%)	0 (0%)	0 (0%)	0 (0%)	0 (0%)
Others (45%)	16	8 (34%)	6 (29%)	8 (42%)	4 (25%)	19 (58%)	16 (21%)	12 (54%)	3 (16%)
Total (100%)	35	23 (64%)	21 (58%)	19 (52%)	16 (46%)	33 (100%)	26 (78%)	22 (42%)	10 (30%)

Using the resection specimen as gold standard, accuracy of diagnosis including both the subtype and the grade was 90% for core needle biopsies and 91% for open biopsies. In both groups sampling was the most important reason for discrepancy. The number of immunostains done on core biopsies where FISH was done were substantially less (0-3) versus an average of 5 in cases without FISH.

Conclusions: Core needle core biopsies have similar rates of diagnostic accuracy as open biopsies. FISH is a useful adjunct in diagnosis of sarcomas and increases the reliability of diagnosis especially in fatty, round cell and certain benign and intermediate vascular tumors. In addition FISH reduces the number of immunostains needed. The increased cost, time and morbidity of open biopsy can be avoided and should be reserved only for cases where core needle biopsy has failed.

68 Craniofacial Chondromyxoid Fibromas: Clinicopathologic Analysis of 23 Cases

David M Meredith, Christopher DM Fletcher, Vickie Y Jo. Brigham and Women's Hospital, Boston, MA.

Background: Chondromyxoid fibroma (CMF) is a rare benign tumor, usually arising in the metaphyseal region of long bones in young adults. Occurrence in the craniofacial region presents a diagnostic challenge given its rarity and resemblance to malignant mimics. Here we describe clinicopathologic data of 23 cases.

Design: 23 cases identified between 1999-2016 were retrieved from routine and consultation files. H&E and immunohistochemical stains were examined. Clinical/follow-up data were obtained from referring pathologists.

Results: Patients were 12 men and 11 women, median age 44 years (range 5-83). None were known to have inherited syndromes. All patients had solitary lesions. Bones involved were sphenoid (8), ethmoid (4), maxilla (2), occipital (2), nasal septum (2), palatine (2), temporal (2), and undisclosed skull (1). Lesions ranged in size from 0.8 to 6.0 cm (median 2.0). Of the 15 tumors with available radiology, 10 appear to arise on the bone surface with expansion into adjacent sinuses; 5 were intraosseous. Bone erosion/destruction was present in most (12/14) cases, and 6/9 showed calcification on imaging. Microscopically, most tumors showed a lobulated growth pattern with hypocellular central chondromyxoid areas and peripheral hypercellularity, though many were fragmented. Tumor cells had ovoid to tapered nuclei and abundant pale eosinophilic cytoplasm, frequently with stellate processes. Mitoses ranged from 0-2 per 10 HPF (median count 0). No tumors had necrosis. Significant atypia or hyperchromasia were absent except in 1 recurrent tumor previously radiated. Bone invasion was present in 11/22 cases. Focal calcification was evident in 13/22. Other features included foci of hyaline cartilage (2 cases), prominent vacuolization (2), and vascular hyalinization (3). SMA was positive in 6/6 cases. All tumors were negative for keratin and GFAP (0/21), with multifocal EMA in 5/21 cases. S100 was positive in 2/21. Most patients received piecemeal excision or curettage (5/5 positive margins when reported). Follow-up data is available for 10 patients thus far, with local recurrence in 4.

Conclusions: Craniofacial CMF is rare with a high rate of misdiagnosis given aggressive radiologic features and overlapping morphology with malignant mimics. Tumors show diffuse positivity for SMA and infrequent positivity for S100 and EMA. Expression of keratins and GFAP is universally negative. Recurrence is frequent, largely due to the difficulty of obtaining clear surgical margins. Furthermore, these tumors exhibit a propensity for locally destructive and invasive growth, creating significant morbidity in some cases.

69 Whorling Cellular Perineurioma: An Undescribed Variant Mimicking Monophasic Fibrous Synovial Sarcoma

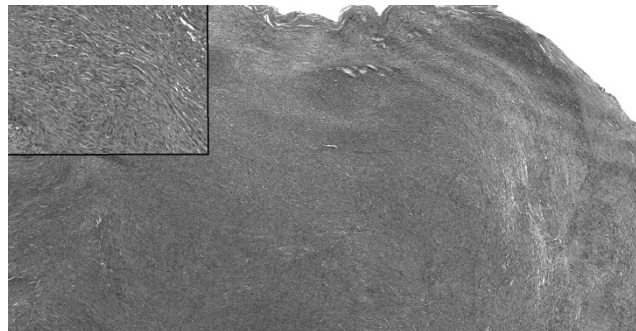
Michael Michal, Dmitry V Kazakov, Abbas Agaimy, Kvetoslava Michalova, Faruk Skenderi, Semir Vranic, Michal Michal. Charles University, Medical Faculty and Charles University Hospital Plzen, Plzen, Czech Republic; Friedrich-Alexander University Erlangen-Nürnberg, Erlangen, Germany; Clinical Center, University of Sarajevo, Sarajevo, Bosnia and Herzegovina.

Background: Synovial sarcoma (SS) is a malignant tumor most commonly arising in the soft tissue of extremities. Monophasic fibrous variant (MSS) is the most frequent of the four SS subtypes. Its differential diagnosis is quite challenging, encompassing a

broad spectrum of neoplasms. We have encountered another potential mimicker which, based on morphology, immunohistochemistry (IHC) and electron microscopy (EM) was shown to consist of perineurial cells. To our knowledge, this perineurioma subtype is not currently recognized. Based on the bland morphology, low proliferative index (PI, Ki67), absence of mitoses and limited follow-up (FU), we propose the term whorling cellular perineurioma (WCP) for these tumors.

Design: Four cases of WCP have been collected from the authors' files. The tumors were analyzed using light microscopy, IHC, fluorescence in situ hybridization (FISH) and EM.

Results: The patients were 3 men and 1 female. The age ranged from 15-61 years (mean: 44 years). Tumors were located on sole, lower jaw, palm and foot. All tumors had an identical, monotonous appearance. The perineurial cells created a confluent, cellular whorls, with only focally discernible long, slender cytoplasmic processes typical for perineurial differentiation. The cells had rounded or slightly elongated nuclei without significant nuclear atypia. Atypical mitoses were absent (inset).



The PI was 1-3%. All tumors were positive with EMA, Claudin-1, GLUT-1 and negative with TLE-1. In 3 cases tested by FISH, none showed alterations of the SYT gene locus. One case analyzed by EM showed characteristic features of perineurial differentiation. FU was available for two patients, both of which showed no signs of recurrence/metastasis after 8 years and 6 months of FU respectively.

Conclusions: WCP represents a distinct subtype of perineurioma, belonging to the benign spectrum of these tumors. The most significant feature of WCP is its potential to be mistaken for MSS. Distinction between these two tumors is of utmost clinical significance.

70 Lipoblasts in Spindle Cell and Pleomorphic Lipomas: A Close Scrutiny

Michael Michal, Dmitry V Kazakov, Ladislav Hadravsky, Kvetoslava Michalova, Petr Grossmann, Petr Steiner, Valentina Renda, Saul Suster, Michal Michal. Charles University, Medical Faculty and Charles University Hospital, Plzen, Czech Republic; Charles University, Third Medical Faculty and Charles University Hospital Kralovske Vinohrady, Praha, Czech Republic; MCW Cancer Center, Medical College of Wisconsin, Milwaukee, WI.

Background: Spindle cell lipomas (SCL) and Pleomorphic lipomas (PL) are distinct soft tissue tumors creating a morphologic continuum with SCL on one side and PL on the other, more atypical side of the spectrum. Besides bizarre, pleomorphic stromal cells, PL often contain a variable number of lipoblasts (LPB), thus occasionally causing diagnostic difficulties. Although the seminal paper on PL by Shmookler and Enzinger mentioned occurrence of LPB in PL in approximately 50% of cases, many modern reports fail to acknowledge this important feature of PL. This situation is even more confusing in cases of SCL. We have found only three publications acknowledging the presence LPB in these tumors. However, in our practice, we have come across many cases of PL but also of SCL with a prominent admixture LPB. This compelled us to review a series of SCL/PL cases from our files in order to more precisely define the frequency of LPB in these tumors, using modern auxiliary methods.

Design: 91 and 38 cases of SCL and PL respectively were retrieved from the author's consultation files and examined microscopically for LPB. When more than 3 unequivocal LPB were found, the case was considered positive. Immunohistochemistry for CD34 and Retinoblastoma (Rb) protein was performed. Cases were also molecular-genetically (MG) tested for MDM2 and CDK4 amplifications and FUS rearrangements.

Results: The patients were 14 women and 47 men, the rest was of unknown gender. CD34 was expressed in all analyzable cases, while Rb protein was consistently deficient. MG results, when available, were in concordance with the morphological diagnosis of SCL/PL. LPB were found in 37 (41%) cases of SCL and 25 cases of PL (66%).

Conclusions: LPB are present in approximately half cases of SCL and two thirds of PL. While in many cases they are inconspicuous, in some others they constitute a very prominent component of the tumor. It is important to be aware of this fact, in order to base the diagnosis on other, diagnostically more important features of SCL/PL and to avoid misinterpretation as liposarcoma.

71 Upregulated BCL2 Expression as a Diagnostic Marker of Spindle Cell/Pleomorphic Lipoma with Deletion of *MiR-15a/16-1* Gene Locus at 13q14

Toru Motoi, Akihiko Yoshida, Masumi Ogawa, Fumie Kakizaki, Ikuma Kato, Akiko Tonooka, Shinichi Horiguchi, Tomotake Okuma, Takahiro Goto, Tsunekazu Hishima. Tokyo Metropolitan Cancer and Infectious Diseases Center Komagome Hospital, Tokyo, Japan; National Cancer Center Central Hospital, Tokyo, Japan.

Background: The diagnosis of spindle lipomas/pleomorphic lipomas (SLs) can be challenging due to their divergent histology, and they need to be distinguished mainly from various lipogenic tumors. SLs are cytogenetically characterized by 13q14 deletion. Although loss of retinoblastoma protein (Rb) expression has been suggested as an indicator of 13q14 deletion, its interpretation is not straightforward in some cases. Because microRNA (miR)-15a/16-1 at 13q14 targets BCL2, and BCL2 upregulation plays a crucial role in hematological malignancies with 13q14 deletion, we tested diagnostic potential of BCL2 in SLs and related tumors.

Design: Formalin-fixed paraffin-embedded samples of 28 SLs, 1 cellular angiofibroma (CAF), and 2 mammary-type myofibroblastomas (MFs) were subjected to immunohistochemistry using antibodies against BCL2 and Rb. Ten each cases of well- and dedifferentiated liposarcomas (WLSs and DLSs) and 5 lipomas (LPs) were used as references. Immunostaining of spindle and/or pleomorphic cells was scored as 3+ or 2+ when at least focal strong positivity was observed in $\geq 50\%$ or 10%-50% of cells, respectively; and it was scored as 1+ or 0, when weak positivity was observed in $\geq 10\%$ or $< 10\%$ of cells, respectively. The reactivity was deemed significant in the cytoplasm for BCL2 and in the nucleus for Rb. Deletion of *miR-15a/16-1* was investigated in 21 SLs, 1CAF and 2MFs by chromogenic in situ hybridization (CISH) using *miR-15a/CEN13q* probes. *miR-15a/16-1* was judged to be deleted when $>30\%$ of cells lacked miR-15a signals by evaluating 100 nuclei.

Results: BCL2 expression (3+) was detected in 21/28 (75%) of SLs and all related tumors. All reference tumors except 2 DLSs (2+ in dedifferentiated component) were negative (0) for BCL2. Complete loss of Rb was observed in 18/28 (64%) of SLs. All W- and DLSs retained Rb expression (3+ or 2+); however, 3/5 (60%) of LPs lacked Rb expression. By CISH, deletion of *miR-15a/16-1* was observed in 19/21 (90%) of SLs and 1/2 (50%) of MFs. Notably, BCL2 expression was absent in 2 SLs in which *miR-15a/16-1* was intact, suggesting their close relationship.

Conclusions: BCL2 expression can be used as a marker of SLs with 13q14 deletion. BCL2 is more widely applicable to differential diagnosis of lipogenic tumors than Rb, including LPs. Upregulated BCL2 may play a role in the pathogenesis of SLs.

72 Clinico-Pathologic Study of ATRX and Notch Receptor Expression in a Large Series of Angiosarcomas

Gauri Panse, Davis R Ingram, Samia Khan, Khalida Wani, Alexander J Lazar, Wei-Lien Wang. The University of Texas M D Anderson Cancer Center, Houston, TX.

Background: Multiple genetic abnormalities have been described in angiosarcomas (AS) including *ATRX* (α -thalassaemia/mental retardation syndrome X-linked), *NOTCH1* and *NOTCH2* mutations. Inactivation of *ATRX* is most frequent in hepatic AS. Notch1 is expressed in normal endothelial cells and 77% of AS. Murine models have shown that inhibition of Notch signaling can induce hepatic and subcutaneous vascular tumors, indicating a tumor suppressive role of Notch pathway in AS. We evaluated the immunohistochemical expression of ATRX and Notch pathway receptors Notch1 and Notch2 in a large cohort of AS and studied their clinico-pathologic significance.

Design: Slides from a clinically annotated tissue microarray and whole slide sections comprising of 135 cases of AS (22 cutaneous, 19 primary breast, 30 post-radiation breast, 32 visceral, 15 deep soft tissue, 7 chronic lymphedema associated, 6 primary bone and 4 AS arising in other sarcomas) were stained for ATRX (Sigma-Aldrich, HPA001906), Notch1 (Abcam, ab27526) and Notch2 (Abcam, ab8926) antibodies. Loss of ATRX expression was defined as $< 10\%$ labelling within the tumor cells while Notch1 & Notch2 were assessed for intensity (0-3) and percentage of tumor cells labelling (0-100%).

Results: ATRX loss was seen in 8/126 cases (5/15 soft tissue, 2/22 cutaneous and 1/23 visceral) and was more frequent in deep soft tissue AS compared to cutaneous, breast or visceral sites ($p < 0.05$). ATRX loss was more common in AS with epithelioid morphology than spindle or vasoformative features ($p = 0.08$). Weak Notch1 expression ($\leq 1+$ intensity) was seen in 29/128 (23%) of AS and more frequently associated with cutaneous site of origin ($p < 0.05$). 18% of primary AS had weak Notch1 expression compared to 40% of advanced disease ($p = 0.012$). Two cases with known Notch1 mutation showed decreased (1+) labelling. Notch2 expression was present in the vast majority of AS with only 4/107 cases (1 cutaneous, 3 visceral) showing complete loss of expression.

Conclusions: ATRX loss was seen in 6% of AS and was more frequent in AS of deep soft tissue (33%) and cases with epithelioid morphology. Decreased Notch1 expression was seen in AS associated with cutaneous origin and advanced disease. These findings suggest that ATRX and Notch pathway may play a role in the pathogenesis of a subset of angiosarcomas.

73 Specificity of H3K27Me3 Loss in Malignant Peripheral Nerve Sheath Tumors

Melike Pekmezci, Areli K Cuevas-Ocampo, Arie Perry, Andrew E Horvai. University of California San Francisco, San Francisco, CA.

Background: Loss of trimethylation at lysine 27 of histone 3 (H3K27me3) has been reported in malignant peripheral nerve sheath tumor (MPNST). Whether H3K27me3 loss is also present in two morphologic mimics of MPNST, synovial sarcoma (SS) and fibrosarcomatous dermatofibrosarcoma protuberans (FS-DFSP), remains controversial. The aim of this study is to evaluate the specificity of H3K27me3 loss for MPNST compared to SS and FS-DFSP.

Design: 119 primary tumors were identified from departmental archives. The diagnoses were based on morphology, immunohistochemical profile and genetic findings using WHO classifications. H3K27me3 immunohistochemistry (Cell Signaling, C36B11, 1:50) was scored by two pathologists, independently based on fraction of cells with nuclear staining: 0: $\leq 5\%$ of tumor cells; 1+: $> 5\%$ but $< 50\%$; 2+ ≥ 50 but $< 95\%$; 3+ $\geq 95\%$. **Results:** 70 SS, 39 MPNST and 10 FS-DFSP were included. H3K27me3 immunohistochemistry is summarized in Table 1.

H3K27me3 IMMUNOSTAINING RESULTS				
	0	1+	2+	3+
SS (n=70)	6(9%)	10(14%)	34(49%)	20(29%)
Monophasic (n=51)	6(12%)	6(12%)	25(49%)	14(27%)
Biphasic (n=17)	-	3(18%)	9(53%)	5(29%)
Poorly differentiated (n=2)	-	1(50%)	-	1(50%)
MPNST (n=39)	17(44%)	6(15%)	4(10%)	12(31%)
NF1-associated (n=26)	13(50%)	6(23%)	-	7(27%)
Sporadic (n=13)	4(31%)	-	4(31%)	5(38%)
FS-DFSP (n=10)	1(10%)	3(30%)	3(30%)	1(10%)

Complete absence of H3K27me3 staining was significantly more common in MPNST than SS ($p < 0.001$, sensitivity = 44%, specificity = 91%). All synovial sarcomas with complete H3K27me3 loss were monophasic; however, this was not statistically significant ($p = 0.22$). While complete loss of H3K27Me3 is also more common in MPNST than FS-DFSP, the difference is only nearly significant ($p = 0.07$). No significant difference between NF-1 associated and sporadic MPNSTs ($p = 0.32$) is observed with respect to loss of H3K27Me3. Decreased H3K27Me staining (1+ or 2+) does not distinguish MPNST from either SS or FS-DFSP.

Conclusions: Complete loss of H3KMe3 is seen in approximately half of MPNST, but is very rare in SS and therefore provides good specificity for the diagnosis of MPNST over SS. A larger number of FS-DFSP may be required to determine H3K27Me3 specificity for this diagnosis. Partial loss of H3KMe3 can be seen in all three tumors and is probably not diagnostically useful in this differential.

74 Composite Hemangioendothelioma (CHE) with Neuroendocrine (NE) Marker Expression: An Aggressive Variant

Kyle D Perry, Alyaa Al-Ibraheemi, Brian P Rubin, William R Sukov, Jin Jen, Hongzheng Ren, Jang Jin, Asha Nair, Jaime Davila, Stefan Pambuccian, Andrew E Horvai, Henry D Tazelaar, Andrew L Folpe. Mayo Clinic, Rochester, MN; Cleveland Clinic, Cleveland, OH; Boston Children's Hospital, Boston, MA; Loyola Medical Center, Maywood, IL; UCSF, San Francisco, CA.

Background: Aberrant expression of NE markers is extremely rare in endothelial neoplasms, with only a single report of 3 such cases. Although most of the tumors in this previous series were originally classified as conventional angiosarcomas (AS), re-review of these and other similar cases has shown them to have mixed retiform and epithelioid features, as seen in CHE, a very rare hemangioendothelioma variant. The natural history and genetic underpinnings of CHE showing NE marker expression have not been previously studied.

Design: All available materials from 9 cases of CHE showing NE marker expression were retrieved from our archives. Immunohistochemistry (IHC) for CD31, CD34, FLI-1, synaptophysin, chromogranin, D2-40, ERG, keratin (OSCAR) and CAMTA1 was performed. Total RNA from FFPE sections of five cases were extracted and subjected to whole transcriptome sequencing using the TruSeq RNA Access protocol. Clinical follow-up was obtained.

Results: The tumors occurred in 4 M and 5 F from 14 to 55 years (mean 38) in age and involved both superficial (wrist, ankle, scalp, hip and foot) and deep (periaortic tissues, C5 vertebra, pulmonary vein, and liver) locations. All contained elongated, retiform vascular channels lined by hyperchromatic "hobnail" endothelial cells and areas of solid growth with uniform epithelioid cells. Mitotic activity was typically $< 1/10$ HPF; necrosis and conventional AS were absent. IHC results were: CD31 (7/7), FLI1 (7/7), ERG (6/6), CD34 (2/7), D2-40 (5/7), synaptophysin (8/8), chromogranin A (1/8), CD56 (4/8), keratin (0/8) and CAMTA1 (0/5). Sequencing analysis showed 1 case with *PTBP1-MAML2* and 1 case with *EPC1-PHC2* fusion transcripts; fusion transcripts were not identified in the remaining 3 cases. Follow-up (8 cases) showed 1 patient with local recurrence and 4 with metastases (bone, lung, liver and brain).

Conclusions: We have identified a distinctive subset of CHE showing NE differentiation. Although the morphological features of these tumors are characteristic of CHE, they more often involve deep locations and display more aggressive behavior than has been typically described. Additionally, they exhibited unique gene fusions not previously identified in any vascular neoplasms. Additional studies are required to determine the precise relationship between the lesions described in this series and conventional CHE.

75 Adrenal Schwannomas: A Clinicopathologic Study with Identification of a Peculiar Hybrid Schwannian/Neuroendocrine Adrenal Medullary Tumor

Kyle D Perry, Andrew L Folpe, Andrew E Horvai, Michael Michal, Michal Michal, Lester DR Thompson, Gretchen Galliano, Ali G Saad, Richard Trepeta, Jorge Torres-Mora. Mayo Clinic, Rochester, MN; Charles University Hospital Plzen, Plzen, Czech Republic; Woodland Hills Medical Center, Woodland Hills, CA; D. of Pathology, S.F., CA; Ochsner Medical Center, New Orleans, LA; UMC, Jackson, MS; St. Joseph's Hospital, Phoenix, AZ.

Background: Adrenal gland schwannomas are rare benign peripheral nerve sheath neoplasms. Given the limited assessment of these tumors in larger multi-institutional cohorts, we reviewed our experience with these tumors and identified an unusual adrenal medullary neoplasm that shows hybrid Schwann cell/neuroendocrine differentiation.

Design: Slides from fifteen consecutive cases with the location of "adrenal" and diagnosis of "schwannoma" were retrieved. Age, site, gender, clinical diagnosis and microscopic features such as cellularity and mitosis were noted. Immunohistochemistry (IHC) for S100, N2F11, CD56, chromogranin, synaptophysin, GFAP, CD117, SOX-10 and Ki-67 was performed, and clinical follow-up was obtained.

Results: The tumors occurred in 4 M and 10 F from 27 to 77 years (mean 57) in age and measured 1 to 18 cm (median 5 cm). Histologically, they were predominantly composed of a more cellular, (Antoni A) component (median of 90%), and proliferation was limited to 0-1 mitoses (per 10 hp). IHC results were: S-100 (13/13), SOX-10 (13/13), CD56 (12/13), and GFAP (8/13). Of the eleven patients with follow-up (ranging from 0 to 176 months, mean of 42 months), none experienced recurrent disease. Within this group, three (two female and one male, 39, 58 and 47 years old) seemed to arise from the adrenal medulla and showed a unique fascicular and nested arrangement of spindle cells exhibiting round to ovoid nuclei, focal epithelioid features and focal microcystic architecture with associated myxoid material. In addition to staining with S-100 and SOX-10, two of these three cases expressed synaptophysin, and three were positive for CD56.

Conclusions: The adrenal schwannomas reviewed largely exhibited clinical, morphologic and immunophenotypic features similar to their soft tissue counterparts. However, a small subset displayed a unique fascicular and microcystic morphology and hybrid schwann cell/neuroendocrine immunophenotype that could represent a variant form of schwannoma. Alternatively, this subset of lesions could be part of the morphologic spectrum of the so-called sustentaculomas of the adrenal gland.

76 Atypical Lipomatous Tumor/Well-Differentiated Liposarcoma (ALT/WDL) and Dedifferentiated Liposarcoma (DDLPS): An Institutional Study of 81 Cases Focusing on the Sclerosing Pattern

Kyle D Perry, Karen Fritchie. Mayo Clinic, Rochester, MN.

Background: ALT/WDL and DDLPS are notorious for recurrence with rates reported up to 91% in the retroperitoneum. Tumors with hypocellular fibrous areas are classified as the sclerosing variant of ALT/WDL rather than DDLPS even though they contain large zones devoid of lipogenic differentiation. We aimed to better characterize the behavior of tumors harboring this pattern.

Design: Cases of ALT/WDL and DDLPS were retrieved from our institutional archives (1992-2015). Recurrent/treated tumors were excluded. The following patterns were catalogued and quantified if they filled >90% of a low power field (LPF=4x objective field): sclerosing, low-grade spindle cell, high-grade sarcoma and myxoid. Tumors harboring ≤5 LPFs of the sclerosing pattern without any other pattern were classified as ALT/WDL. Cases were designated as "sclerosing-rich" if they contained >5 LPFs of the sclerosing pattern without other patterns. The remaining tumors were considered "DDLPS." Clinical features/outcomes were analyzed.

Results: 81 primary untreated tumors (50M, 31F; 39-88 years; 2-59 cm) occurred at the following sites: retroperitoneum (RP)/groin (n=45), extremity (n=31), head/neck (n=3) and mediastinum (n=2). 56 cases (69%) were classified as ALT/WDL, 10 (12%) as "sclerosing-rich" and 15 (19%) as DDLPS. 14 of 81 (17%) patients experienced an adverse event (AE) (recurrence=13, metastasis=1). The rate of AE for ALT/WDL, sclerosing-rich and DDLPS was 11% (6/55), 30% (3/10) and 33% (5/15), respectively. Although there was a trend toward worse outcome for patients with sclerosing-rich vs. ALT/WDL, this was not significant (p=0.14). However, a significant increase in AE was observed with DDLPS (p=0.04). Of tumors occurring in the RP/groin/mediastinum (n=47), the rate of AE for ALT/WDL, sclerosing-rich and DDLPS was 16% (4/25), 38% (3/8) and 36% (5/14), although the differences did not reach statistical significance. Comparing outcome by site, AE were identified in 26% (12/47) of cases in the RP/groin/mediastinum vs. 6% (2/34) of extremities/head/neck tumors (p=0.03). Follow-up ranged from 0 to 166 months (median 49), and the median time to AE was 26.5 months (range 7 to 48).

Conclusions: We confirm prior work that DDLPS, as well as tumors arising in the RP/groin/mediastinum, behave more aggressively, even though the recurrence rate at these sites may be less than previously reported. This data suggests that sclerosing-rich tumors may also be at increased risk for AE compared to ALT/WDL.

77 Novel NF1-TEK Fusion in Giant Cell Tumor of Bone

David J Pisapia, David C Wilkes, Patrick J McIntire, Kyung Park, Andrea Sboner, David S Rickman, Rohan Ramakrishna, Mark A Rubin, Juan Miguel Mosquera. Weill Cornell Medical College, New York, NY.

Background: Giant cell tumor of bone (GCTB) is a low-grade neoplasm that can be locally aggressive and has the potential to metastasize. Its genetic hallmark remains unknown and it is debatable if mononuclear and giant tumor cell populations are both neoplastic.

Design: We studied a GCTB arising in the temporal bone of a 28-year-old male who was referred to the Precision Medicine clinic. Whole exome sequencing did not reveal targetable mutations or somatic copy number alterations. RNA-seq data was analyzed by FusionSeq and FusionCatcher. An additional 7 GCTB, 21 giant cell tumors of soft tissue (GCTST) and 5 aneurysmal bone cysts (ABC) were screened by FISH. TEK immunohistochemistry (IHC) was performed on a subset of GCTB cases.

Results: An *NF1-TEK* fusion candidate was detected in the index case and validated by FISH and RT-PCR, demonstrating fusion of *NF1* exon 26 to *TEK* exon 12 at the site of a shared fibronectin type-3 protein domain. Evidence for *TEK* rearrangement was identified by FISH in 5 additional GCTB. Both mononuclear and giant cells in GCTB demonstrated strongly positive membranous immunoreactivity for TEK. GCTST and ABC cases were negative for *TEK* rearrangement. TEK (also known as TIE2) is a cell surface tyrosine kinase receptor that binds angiotensin and has been implicated in angiogenesis. Moreover, studies have shown that it is expressed in a subset of circulating monocytes and that it may be significantly upregulated in tumor associated macrophages. Further confirmation of this fusion gene within a larger cohort of GCTB cases is underway as are functional validation studies.

Conclusions: We describe a novel gene fusion involving *FNI* and *TEK* in GCTB that is associated with TEK overexpression in tumor cells. This finding may lead to further insights into monocytic expression of TEK and the pathogenesis of GCTB as well as provide a useful aid in diagnostically difficult cases. Moreover, the discovery of this chimeric protein may have significant clinical impact by providing a potential therapeutic target.

78 Pseudomyogenic Hemangioendothelioma of Bone and Soft Tissue – A Clinicopathologic, Immunohistochemical and Fluorescence In Situ Hybridization Study of 7 Cases

Dinesh Pradhan, Richard L McGough, Karen E Schoedel, Sarangarajan Ranganathan, Uma NM Rao. University of Pittsburgh Medical Center, Pittsburgh, PA.

Background: Pseudomyogenic hemangioendothelioma (PHE) is an uncommon neoplasm with propensity for local recurrence. Synchronous bone and soft tissue involvement can occur in a small percentage of cases. Primary bone lesions are very rare.

Design: 7 cases of PHE were retrieved from the archives of the department of pathology. The outcome information was available in five cases. Fluorescence in situ hybridization (FISH) studies were performed to detect *c-myc* amplification and (7;19)(q22;q13) translocation.

Results: Of the 7 cases, 6 were male and 1 female patient (M:F ratio of 6:1). The median age of the patients was 24 years (range 9-53 years). The tumor sizes ranged from 0.3- 6 cm (mean=1.3 cm). In 6 cases the tumors were located in the lower limb bone and soft tissue while in 1 case the upper extremity was involved. The tumor was multifocal in 4 cases. In 3 cases there was simultaneous bone and soft tissue involvement. 3 patients had bone involvement only and 1 patient had subcutis tumor only. The tumors were composed of loose fascicles and sheets of plump spindle or epithelioid cells with ample eosinophilic cytoplasm and vesicular nuclei with prominent to inconspicuous nucleoli. Mitosis averaged 1 per 10 HPF. Immunohistochemical stains revealed all tumors to be positive for AE1/AE3 (7/7), ERG (6/6) and FLI-1 (6/6). Most of the tumors were variably positive for CD31 (6/7), CAM5.2 (2/3) and SMA (4/6). INI1 was conserved in the one case in which it was performed. All cases were negative for CD34, desmin and S-100. Ki67 proliferation index varied from 5%-20%. No *c-myc* amplification was detected by FISH in any of the five cases analyzed (0/5). Interphase FISH for (7;19)(q22;q13) translocation detected fusion in only one case (Subcutaneous PHE) out of the 4 cases analyzed successfully (25%). In 3 other cases the abnormal fusion pattern was detected in a few cells but was insufficient for a positive result. All the 4 cases revealed hyperploidy with polysomy of both the chromosome 7 and 19 in 4-39% of cells. 4 patients underwent excision and 1 (multifocal bone and soft tissue tumor) needed below-knee amputation. All the five patients with outcome information were alive and free of disease after a mean follow-up period of 42 months.

Conclusions: PHE is a rare indolent neoplasm that should be distinguished from epithelioid hemangioendothelioma and epithelioid sarcoma. Long term follow-up is warranted.

79 Immunohistochemical Evaluation of Chromatin Regulatory Gene Surrogates in Chordoma

Daniel C Ramirez, Lu Wang, Khedoudja Nafa, Patrick Boland, Meera Hameed. Memorial Sloan Kettering Cancer Center, New York, NY.

Background: Chordoma is a rare primary bone neoplasm typically arising within the adult spine that shows aggressive local behavior, has a propensity for local recurrence after gross total resection, and can metastasize to distant sites. Utilizing next generation sequencing on twenty-four patient samples we have shown that while chordoma has an overall low mutation rate, approximately 40% of mutational events affected chromatin regulatory genes, most notably SETD2, a gene encoding a histone methyltransferase.

Design: Forty formalin-fixed paraffin-embedded (FFPE) patient samples with typical histopathologic features of conventional chordoma with adequate tumor content were selected for construction of tissue microarray (TMA) followed by immunohistochemical staining for selected chromatin regulation associated proteins and surrogates: INI-1, H3K27me3, and H3K36me3.

Results: The chordoma samples reviewed arose primarily from the sacrococcygeal area (38 cases), one case arose from the lumbar spine, and one from the cervical spine. All patients were adults (24-80 years old, median age 54) with 31 males and 9 females. At the time of last follow up, 23 patients were alive with no evidence (NED) of disease, 6 patients were alive with disease (AwD), 10 patients have died of their disease (DoD), and one patient has had multiple treated recurrences with no current evidence of disease.

Table below summarizes the results:

	Loss of IHC Staining				
	INI-1	H3K27me3	H3K36me3		
NED (24 patients)	2 (8%)	1 (4%)	0	0	0
AwD (6 patients)	0	2 (33%)	0	1 (17%)	0
DoD (10 patients)	0	2 (20%)	0	0	1 (10%)
Total (40 patients)	2 (5%)	5 (12.5%)	0	1 (2.5%)	1 (2.5%)

Conclusions: The interactions between chromatin regulatory genes appear to play a role in chordoma pathogenesis. In this small group of patients, abnormal H3K27me3 expression is associated with poor outcome. A larger study is underway to verify the above findings.

80 Differential Expression of Specific Skeletal Muscle Markers in a Series of 300 Rhabdomyosarcomas, Including Various Subtypes

Barat Rekhii, Chhavi Gupta, Girish Chinnaswamy, Tushar Vora, Sajid Qureshi, Jyoti Bajpai, Nehal Khanna, Siddhartha Laskar. Tata Memorial Centre, Mumbai, Maharashtra, India; Tata Memorial Centre, Mumbai, Maharashtra, India; Tata Memorial Centre, Mumbai, Maharashtra, India.

Background: Recent WHO classification includes spindle cell/sclerosing as another subtype of rhabdomyosarcoma(RMS). Earlier, few studies have shown diagnostic and prognostic value of skeletal muscle specific markers, such as myogenin in cases of alveolar RMS.

Design: This study aimed at evaluating the differential expression and prognostic value of myogenin and MyoD1 in 300 cases of RMS, including 140 cases(46.7%) of ARMS, 90 of ERMS(30%), 61(20.3%) of spindle cell/ sclerosing RMSs and 9 cases(3%) of pleomorphic RMS. Immunohistochemical expression of myogenin and MyoD1 was graded on the basis of percentage of tumor cells displaying positive intranuclear immunostaining, such as grade 1(1-25%); grade 2(26-50%); grade 3(51-76%) and grade 4 (76-100%). Outcomes/ follow-up details were available in 272 (90.7%) patients. Various clinicopathologic features were correlated with 3-year disease-free and overall survival.

Results: Overall, desmin was expressed in 292/299(97.6%) cases, myogenin in 238/267(89.1%) and MyoD1 in 192/266(72.2%) cases of RMS. High myogenin expression (more than, equal to 51% positive tumor cells) was significantly associated with cases of alveolar RMS(ARMS) (95/121,78.5%), as compared to other subtypes(48/117, 41%). ($p < 0.001$). High MyoD1 expression ($\geq 51\%$ tumor cells) was seen in more cases of pure sclerosing, combined with spindle cell/ sclerosing RMSs(10/10, 100%), as compared to the other subtypes(91/141, 67.4%) ($p = 0.032$). Among 212 cases, where both, myogenin and MyoD1 immunostaining was performed, only myogenin positivity was seen in most cases of ARMS(34/47, 72.3%) and only MyoD1 positivity was seen more in most cases spindle cell/ sclerosing RMS(14/20, 60%), compared to other subtypes ($p < 0.001$). There was no significant difference between high myogenin expression and disease-free survival and/ or 3 year overall survival. Children, especially in first decade; patients with tumor size < 5 cm; without metastasis and with early tumor stage, showed relatively better survival outcomes.

Conclusions: This study reinforces significant association between high myogenin expression and cases of ARMS, as compared to other subtypes. High MyoD1 expression was seen more in cases of spindle cell/sclerosing RMSs, compared to other subtypes. Overall, high myogenin expression was not found to be associated with aggressive clinical outcomes.

81 Neurofibromin C Terminus-Specific Antibody (clone NFC) Identifies NF1-Inactivated GIST

Sabrina Rossi, Daniela Gasparotto, Matilde Cacciatore, Maurizio Polano, Monia Niero, Alessia Mondello, Marta Sbaraglia, Erica Lorenzetto, Alessandra Mandolesi, Alessandro Gronchi, David E Reuss, Andreas von Deimling, Roberta Maestro, Angelo P Dei Tos. Treviso General Hospital, Treviso, Italy; CRO Aviano NCI, Aviano, Italy; University of Marche, Ancona, Italy; INT Milano NCI, Milano, Italy; University of Heidelberg, Heidelberg, Germany.

Background: NF1 inactivation is involved in the pathogenesis of GIST arisen in the context of Neurofibromatosis type 1. A high frequency of *NF1* mutations has been recently reported in "apparently sporadic" *KIT/PDGFR* wild-type GIST. *NF1* mutation in GIST has prognostic and predictive implications. We sought to assess the efficacy of an in house-generated monoclonal antibody directed against neurofibromin C-terminus (NFC) in detecting *NF1* gene inactivation in the context of GIST.

Design: The study was carried out on formalin-fixed paraffin-embedded tissue samples of 84 GIST fully profiled for *KIT*, *PDGFR*, *BRAF*, *SHD* gene status (see table). These included 16 NF1-associated GIST and 37 GIST unrelated to NF1 (*NF1* wild-type or carrying non-pathogenic mutations). Immunohistochemistry was carried out in an automated immunostainer. Cases were scored as NFC negative when no cytoplasmic staining was seen in the neoplastic cells in presence of appropriate internal controls (fibroblasts, ganglion cells, plasmacells, endothelium, smooth muscle). In NFC positive cases, staining intensity (weak, moderate, strong) was recorded.

Results: Results are summarized below:

NF1 association	Evidence	# cases	NFC loss
NF1-associated GIST	Clinical (Neurofibromatosis type 1 clinical diagnosis)	5	4/5
	Molecular (pathogenic/possibly pathogenic <i>NF1</i> mutations)	11	8/11
NF1-unrelated GIST	Molecular (non-pathogenic <i>NF1</i> mutations)	2	0/2
	Molecular (no <i>NF1</i> mutation)	35	1/35
Undetermined	NF1x sporadic GIST (not analyzed for <i>NF1</i> gene status)	31	0/31
TOTAL		84	

NFC immunoreactivity was lost in 4/5 GISTs arisen in clinically diagnosed Neurofibromatosis type 1 patients. NFC was negative also in 8/11 (72.7%) *NF1*-mutated GIST, all carrying *NF1* biallelic inactivation with either large deletions (2 cases) or truncating mutations (4 frameshift, 2 nonsense). NFC reactivity was retained in GIST with mutations of uncertain (1 case) or no pathogenic significance (2 cases), and was weak in 2 cases with a hemizygous nonsense and a homozygous missense mutation, respectively. All but one of the 35 cases that were negative at *NF1* gene mutation analysis were NFC diffusely positive (11 strong, 14 moderate and 9 weak).

Conclusions: NFC antibody efficiently detects *NF1* biallelic gene inactivation (associated to protein truncation or large deletions) in GIST.

82 STAT6 Immunohistochemical Staining in Solitary Fibrous Tumor and Histologic Mimics, a Single Institute Experience

Omer Saeed, Liang Cheng, Shanxiang Zhang, Shaoxiang Chen. Indiana University school of Medicine, Indianapolis, IN.

Background: Neither the morphology nor staining with CD34 is specific for solitary fibrous tumors (SFT). STAT6 stain has proved to be a good surrogate for the genetic alteration (NAB2-STAT6 gene fusion) and showed high sensitivity and almost perfect specificity for SFT. Due to difficulty to use STAT6 polyclonal antibody in our lab, this study is to validate the use of STAT6 rabbit monoclonal antibody in differentiating SFT from the most common histologic mimics.

Design: Fifty cases of SFT and 77 cases from 5 other tumors were stained immunohistochemically using Abcam's STAT6 Rabbit monoclonal (YE361) antibody. Only nuclear staining was considered positive. The staining intensity was classified as strong, intermediate or weak. The extent of immunoreactivity was graded according to the percentage of positive tumor cells (0, no staining; 1+, $< 5\%$; 2+, 5-25%; 3+, 26-50%; 4+, 51-75%; and 5+, 76-100%).

Results: Positive nuclear STAT6 staining was present in 50 SFT cases (50/50, 100% sensitivity) and no nuclear staining was identified in the other cases (synovial sarcoma, 0/17; malignant peripheral nerve sheath tumors, 0/16; undifferentiated pleomorphic sarcoma, 0/25; dermatofibrosarcoma protuberans, 0/10; low grade fibromyxoid sarcoma, 0/9). The STAT6 staining in SFT was usually diffuse (5+ in 21 cases; 4+ in 18 cases; 3+ in 9 cases; and 2+ in 2 cases) and strong (strong in 45 cases; intermediate in 4 cases; and weak in one case).

Conclusions: STAT6 is highly sensitive and specific marker (100%) for solitary fibrous tumors using monoclonal STAT6 antibody and particularly useful in the diagnosis of difficult SFT cases.

83 Primary Pseudomyogenic Hemangioendothelioma of Bone: A Monoinstitutional Retrospective Clinicopathologic and Molecular Analysis of 21 Cases

Marta Sbaraglia, Alberto Righi, Marco Gambarotti, Daniel Vanel, Angelo P Dei Tos, Piero Picci. Rizzoli Orthopaedic Institute, Bologna, Italy; Treviso Regional Hospital, Treviso, Italy.

Background: Pseudomyogenic hemangioendothelioma (PMHE) is a distinctive, locally aggressive rarely metastasizing vascular tumor, mainly described in soft tissue. Few cases of primary PMHE of bone have been reported in the literature so far.

Design: To better define the clinical behavior of PMHE occurring primarily in bone, we reviewed 541 cases of primary bone vascular tumors treated at the Rizzoli Institute from 1901 to 2016.

Results: Morphological, radiological, immunohistochemical and molecular analysis led to the identification of 21 cases primary PMHE of bone. The series included 17 male and four female with a mean age of 33 years (ranging between 12 and 66 years). Fifteen patients had multiple tumors with a distinct regional distribution (12 in the lower extremity, two in the upper extremity, and one in the spine and pelvis). Six patients presented with a single lesion localized in the proximal tibia (2 cases), in a finger, lumbar vertebra, proximal femur and metatarsal bone. Twelve cases (57.1%) showed soft tissue involvement. On imaging all cases were well circumscribed and all but two were lytic and homogeneous. Patients received various treatments (several biopsies and/ or curettage, resection, and amputation) depending on clinical and radiological features. Surgical margins were wide or marginal in resections and amputations. Five patients underwent adjuvant radiotherapy and three patients received adjuvant chemotherapy. Follow-up data were available for all but one patient with a mean of 138 months (ranging between 2 and 288 months). Four patients, treated with curettage, recurred locally. All but three patients were alive without disease at the time of the last follow-up. Three patients were alive with local disease without metastases at the time of last follow-up (three, 17 and 19 months respectively).

Conclusions: PMHE can present as a primary vascular bone tumor. The most important clinical characteristics are the male prevalence, and the multifocality (most often in the lower extremities). A conservative therapeutic approach is recommended in consideration of the tendency to recur or progress locally in absence of systemic spread.

84 Claudin-4 Expression Distinguishes SWI/SNF Complex-Deficient Undifferentiated Carcinomas from Sarcomas

Inga-Marie Schaefer, Abbas Agaimy, Jason L Hornick, Christopher DM Fletcher. Brigham and Women's Hospital, Harvard Medical School, Boston, MA; University Hospital Erlangen, Erlangen, Germany.

Background: Inactivation of subunits of the SWI/SNF chromatin remodeling complex is a feature of select carcinomas and sarcomas with epithelioid morphology and variable keratin expression, making the distinction between carcinoma and sarcoma challenging in some cases. The tight junction-associated protein claudin-4 is a marker of epithelial differentiation that is expressed in nearly all carcinomas. Claudin-4 expression has been reported in the glandular component of biphasic synovial sarcoma but has not been systematically evaluated in other sarcoma types. In this study we assessed claudin-4 expression in SWI/SNF complex-deficient neoplasms showing loss of SMARCB1 (INI1), SMARCA4 (BRG1), or ARID1A and other sarcomas with epithelioid morphology.

Design: Immunohistochemistry was performed using a mouse monoclonal antibody directed against claudin-4 (1:100 dilution; clone 3E2C1; Invitrogen) in 130 neoplasms, including 90 soft tissue tumors with epithelioid morphology and/or SMARCB1 deficiency [20 epithelioid sarcomas (10 conventional, 10 proximal-type); 10 epithelioid angiosarcomas; 10 epithelioid hemangioendotheliomas; 15 epithelioid malignant peripheral nerve sheath tumors; 10 malignant rhabdoid tumors; 15 myoepithelial carcinomas; 10 biphasic synovial sarcomas], 10 ovarian clear cell carcinomas (OCCC), 10 ovarian small cell carcinomas of hypercalcemic type (SCCOHT), and 20 SWI/SNF complex-deficient undifferentiated carcinomas (14 SMARCB1-deficient and 6 SMARCA4-deficient, including rhabdoid carcinomas of various sites and sinonasal carcinomas).

Results: Membranous expression of claudin-4 ($\geq 5\%$ of cells) was observed in all biphasic synovial sarcomas (epithelial component only), all OCCC, and 16 (80%) SWI/SNF complex-deficient undifferentiated carcinomas. All other soft tissue tumors were negative for claudin-4, with the exception of 2 myoepithelial carcinomas and 1 malignant rhabdoid tumor. Interestingly, none of the SCCOHT expressed claudin-4.

Conclusions: Expression of claudin-4 is highly specific for true epithelial differentiation and may be useful to distinguish SWI/SNF complex-deficient undifferentiated carcinomas from sarcomas with epithelioid morphology. The lack of claudin-4 expression in SCCOHT suggests that these tumors may be better classified as sarcomas rather than carcinomas.

85 YAP1 Expression in Different Subtypes of Rhabdomyosarcoma

Ahsan Siddiqi, Sultan Habeebu, Maria Tsokos, Atif Ahmed. University of Missouri Kansas City, Kansas City, MO; Children's Mercy Hospital, Kansas City, MO; Beth Israel Deaconess Medical Center, Boston, MA.

Background: Rhabdomyosarcoma is a common malignancy of skeletal muscle with variable morphology and clinical behavior. Histologically, alveolar, embryonal, spindle cell/sclerosing and pleomorphic subtypes are recognized. YAP1 is a member of the Hippo pathway that is an important transcriptional regulator of muscle development. Few recent reports have highlighted the role of YAP1 in rhabdomyosarcoma carcinogenesis. The purpose of this study is to define the expression of YAP1 in different subtypes of rhabdomyosarcoma and its relation to site and clinical stage.

Design: Duplicate tumor tissue samples, arranged in tissue microarray (TMA) format (US Biomax, Rockville, Maryland), were analyzed for YAP1 expression by immunohistochemistry. Pertinent clinical data included patient age, sex, tumor location, and clinical stage. YAP1 staining was performed with automated immunohistochemistry using antigen retrieval with placenta and medulloblastoma tissues as positive controls. The intensity of the nuclear staining was scored as negative, low (weak staining less than the positive control) or high (staining equal to or stronger than the positive control). The staining intensity was correlated with clinical data and the significance of any associations was statistically analyzed.

Results: Of the total rhabdomyosarcoma cases (n=96), 30 cases (31%) were pleomorphic, 27 (28%) were embryonal, 24 (25%) alveolar and 15 (16%) spindle cell. Ages ranged from 1–91 years with 1.8:1 M/F ratio. High YAP1 staining was identified in the pleomorphic and embryonal and was least common in the alveolar (0%) and spindle cell subtypes (13%). Of the non-alveolar subtypes, high YAP1 staining was more noted in stages 3 and 4 than stage 2 (30% versus 13%; p=0.197). High YAP1 expression was present in 3/3 (100%) of tumors in the bladder, 3/12 (25%) of tumors in the testis and 8/45 (18%) of tumors in the extremities. No YAP1 staining was seen in tumors from the cervix (n=3), uterus (n=2), or vulva (n=1).

Conclusions: These results indicate that YAP1 is important in the tumorigenesis of non-alveolar rhabdomyosarcomas, particularly the pleomorphic and embryonal subtypes. High YAP1 staining may differentiate alveolar from other subtypes. YAP1 expression may also correlate with clinical stage and tumor site. Additional studies with whole slide staining and clinical survival data are needed to further investigate the role of YAP1 in the diagnosis and prognosis of rhabdomyosarcoma tumors.

86 Ossifying Fibromyxoid Tumor: Report of a Case Characterized by a Novel HCFC1-PHF1 Fusion Product

Margaret K Stevenson, David Swanson, Andrew Wong, George Charames, Rita A Kandel, Brendan C Dickson. Mount Sinai Hospital, Toronto, ON, Canada; University of Toronto, Toronto, ON, Canada; Lunenfeld-Tanenbaum Research Institute, Toronto, ON, Canada.

Background: Ossifying fibromyxoid tumor (OFMT) is a rare mesenchymal neoplasm of uncertain origin. Tumors predominate in the extremities and are characterized by a rim of metaplastic bone, distinctive architecture, and S100 immunoreactivity. OFMT is a translocation-associated soft tissue tumor. The majority of cases are reported to contain a gene fusion involving *PHF1* that most frequently partners with *EP400*. Here we describe a case of OFMT containing a novel *PHF1* fusion product.

Design: A 66 year-old male presented with a superficial arm mass. A diagnostic biopsy was performed demonstrating a morphology characteristic of OFMT. Targeted next-generation sequencing was performed for diagnostic confirmation.

Results: Immunohistochemistry was notably negative for S100. Targeted next-generation sequencing revealed an *HCFC1-PHF1* fusion product, which was confirmed with subsequent reverse transcription polymerase chain reaction analysis.

Conclusions: We report *HCFC1-PHF1* as a novel fusion product occurring in OFMT. While most cases of OFMT appear to involve a *PHF1-EP400* translocation event, other *PHF1* partners have been described, including: *MEAF6* and *EPC1*. Interestingly, similar to the current case, the latter fusion products have been reported to be associated with S100 negative tumors. Very recently a number of non-*PHF1* fusion genes have been identified to be associated with OFMT, including: *CREBBP-BCORL1*, *KDM2A-WWTR1* and *ZC3H7B-BCOR*. Further studies are necessary to determine: (1) the extent to which *HCFC1* accounts for reports of *PHF1*-rearranged OFMT lacking an identified fusion partner, and (2) whether this fusion product is shared with other tumors, such as endometrial stromal sarcoma.

87 A Novel CRT1-SS18 Gene Fusion in an Undifferentiated Round Cell Sarcoma- Ewing- Like Sarcoma or Poorly Differentiated Synovial Sarcoma- A Diagnostic Dilemma

VP Sumathi, Abdullah Alhollé, Angela Niblet, Cristina R Antonescu, Farida Latif. Royal Orthopaedic Hospital, Birmingham, United Kingdom; University of Birmingham, Birmingham, United Kingdom; Memorial Sloan-Kettering Cancer Center, New York, NY.

Background: Small blue round cell tumors (SBRCTs), which encompasses Ewing sarcoma (ES), Ewing-like sarcoma (ELS) and poorly differentiated synovial sarcoma (PDSS), are a heterogeneous group of tumours that are diagnostically challenging due to striking morphological and immunohistochemical similarities. In recent years, the emerging group of ELS have shown to carry gene fusions involving *CIC-DUX4*, *CIC-FOXO4*, *BCOR-CCNB3*, *BCOR-MAML3* and *ZC3H7B-BCOR*. In this report we identified a novel gene fusion, *CRT1-SS18*, in a 35 year old man with a soft tissue sarcoma.

Design: A case of ELS that lacked the known translocations for EWS, ELS and SS were identified from the files of our pathology database. High-throughput RNA-seq analysis of both the tumour and corresponding normal sample revealed a novel *CRT1-SS18* somatic gene fusion in the tumour. These findings were confirmed by RT-PCR, long-range PCR and fluorescence in situ hybridization with a split apart of both SS18 and CRT1 custom BAC probes

Results: The patient was a 35 year old man who presented with a rapidly increasing, painless, lump on his right thigh for about 9 months and the imaging findings were suggestive of soft tissue sarcoma.

Grossly, an intramuscular, fleshy tumour measuring 70x65x53mm was observed. Histologically the tumour consisted of solid sheets and nests of small round cells surrounded by desmoplastic stroma reminiscent of desmoplastic small round cell tumour (DSRCT).

Immunohistochemically, the tumours cells were diffusely positive for vimentin and CD99. AE1/AE3 showed focal positivity but was negative for TLE-1 and BCL2.

Conclusions: We present a case of undifferentiated round cell sarcoma with a novel *CRT1-SS18* gene fusion in a 35 year old man with a soft tissue sarcoma of his right thigh which showed striking morphological resemblance to DSRCT. The patient followed an aggressive clinical course with bilateral lung metastases 18 months after diagnosis and death 5 years later. Although the morphology and phenotype favour an undifferentiated small round cell sarcoma, probably Ewing-like sarcoma, further investigation of a large cohort of ELS and poorly differentiated SS cases need to be analysed to determine the incidence and phenotype of *CRT1-SS18* gene fusion.

88 Inflammatory Myofibroblastic Tumor: Expanding the Spectrum of ALK Fusion Partners

David Swanson, Andrew Wong, George Charames, Jeffery J Tanguay, Rita A Kandel, Brendan C Dickson. Mount Sinai Hospital, Toronto, ON, Canada; University of Toronto, Toronto, ON, Canada; Lunenfeld-Tanenbaum Research Institute, Toronto, ON, Canada; Peterborough Regional Health Centre, Peterborough, ON, Canada.

Background: Inflammatory myofibroblastic tumor (IMT) and inflammatory myofibroblastic sarcoma (IMS) are uncommon soft tissue neoplasms of (myo)-fibroblastic differentiation, and characteristically associated with a prominent inflammatory component. Early cytogenetic studies lead to recognition of anaplastic lymphoma kinase (*ALK*) rearrangement in approximately 50% of cases. More recently non-*ALK* genetic drivers have been reported. Using targeted next-generation sequencing we characterize additional cases of *ALK* positive IMT/IMS.

Design: Four cases of IMT/IMS with confirmed *ALK* immunorepression and/or *ALK* rearrangement by fluorescence *in situ* hybridization were identified following a

retrospective review of our archive. RNA was extracted from formalin-fixed paraffin-embedded tissue. RNA-seq libraries were prepared using 20-100 ng total RNA and hybridized to a 507 gene RNA-seq targeted fusion panel. Each sample was sequenced with 76 base-pair paired-end reads on an Illumina MiSeq at 8 samples per flow cell (~3 million reads per sample). The resulting output was analyzed using STAR aligner and Manta fusion caller.

Results: Adequate RNA was obtained in each case. All four tumors were confirmed to contain *ALK* fusion products. In two cases previously reported fusion partners were identified, including *RANBP2-ALK* and *FNI-ALK*. The remaining two cases were found to contain novel *ALK* fusion partners. These products were separately confirmed by reverse transcription polymerase chain reaction testing.

Conclusions: Accurate classification of IMT/IMS is essential since *ALK* fusions represent a potential therapeutic target. More recently non-*ALK* driving mutations have been identified in IMT/IMS (e.g., *ROSI*-, *PDGFRβ*- and *ETV6*-). These, and related, fusion products have further been reported in other tumors-types, including lymphoma, non-small cell lung carcinoma, and pediatric renal cell carcinoma, amongst others. In addition to confirming the occurrence of two previously reported fusion products in IMT, our study adds to an ever-expanding – and overlapping amongst disparate tumour types – list of recognized *ALK* fusion partners occurring in IMT/IMS.

89 Prognostic Significance of TAZ/YAP Activation and p53 Inactivation in Sarcomas

Jon Thomason, Stephanie Ivins, Benjamin Miller, Mohammed Milhem, Munir R Tanas. University of Iowa, Iowa City, IA.

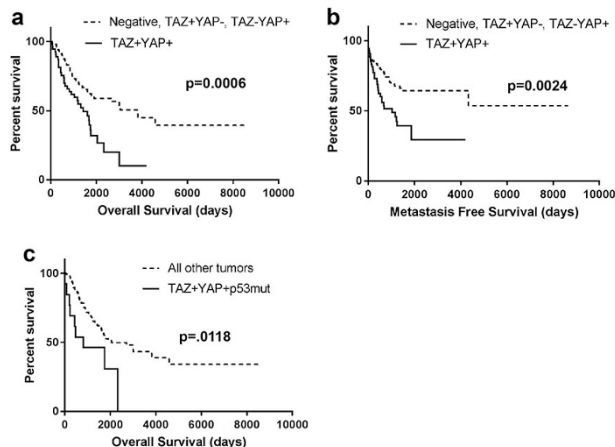
Background: TAZ and YAP are transcriptional coactivators and oncoproteins inhibited by the Hippo pathway. They are activated (nuclear localization) in 66% and 50% of sarcomas respectively. TAZ and YAP expression/activation at the protein level and potential synergy with p53 inactivation in sarcomas has not been investigated. We evaluated 160 sarcomas representing various sarcoma types by immunohistochemistry (IHC) for activation of TAZ and YAP as well as p53 inactivation and correlated with patient overall and metastasis free survival.

Design: IHC for TAZ, YAP and p53 was performed on 160 primary, untreated sarcomas (see Table). TAZ or YAP activation was defined as greater than 70% of cells with at least intermediate level nuclear staining. p53 positivity (p53mut) was defined by at least 5% nuclear immunoreactivity of any intensity, indicating the presence of an underlying p53 inactivating mutation. Patient survival and metastasis data was obtained and Kaplan-Meier analyses were performed.

Results: Combined TAZ and YAP activation resulted in decreased overall survival (median survival 1429 v. 3823 days, $p=0.0006$, Figure 1a), as well as decreased metastasis free survival ($p=0.0024$, Figure 1b). TAZ and YAP activation alone did not impact overall survival. Combined TAZ and YAP activation with concurrent p53 staining resulted in a further decrease in overall survival (median survival 815 v. 2049 days, $p=0.0118$, Figure 1c).

Histological Type	Cases
Rhabdomyosarcoma (Alveolar and adult-type)	11
Angiosarcoma	5
Clear cell sarcoma	4
Chondrosarcoma	17
Dediff liposarcoma (LPS)	8
Epithelioid sarcoma	2
Ewing sarcoma	1
Osteosarcoma	10
Myxoid/round cell LPS	9
Malignant rhabdoid tumor	4
Myxofibrosarcoma	9
MPNST	10
Pleomorphic LPS	7
Synovial sarcoma	11
Leiomyosarcoma	17
UPS	27
Well-diff LPS	8
Total	160

Figure 1



Conclusions: Sarcomas with both TAZ and YAP activation showed decreased overall and metastasis free survival. Overall survival for TAZ/YAP activated sarcomas with concurrent p53 staining was further decreased. These findings suggest that TAZ, YAP and p53 can be used as immunohistochemical prognostic markers in sarcomas. The findings also point to a potential synergistic role between TAZ and YAP, as well as the Hippo pathway and p53 tumor suppressor axes.

90 PAX8 Expression in Sarcomas: An Immunohistochemical Study

George A Tjonas, Andrew E Rosenberg, Daniel P Cassidy, Andre Pinto. University of Miami, Miami, FL.

Background: The expression of PAX8 has been extensively described in normal and neoplastic tissues of the kidney, thyroid, thymus and Müllerian tract. Most studies have shown that PAX8 is a sensitive and specific marker for primary and metastatic carcinomas that arise from these sites. The immunohistochemical expression of PAX8, however, has not been investigated in mesenchymal neoplasms. The goal of this study was to investigate the utility of PAX8 in a variety of sarcomas of bone and soft tissue.

Design: A total of 109 cases corresponding to 23 different diagnoses/subtypes of tumors (see table 1) were reviewed, and immunohistochemistry (IHC) for PAX8 was performed on whole-tissue sections. The IHC was interpreted by 3 pathologists based on the presence or absence of nuclear staining; and intensity of staining graded from 1+ (lowest) to 3+ (highest).

Results: Positive PAX8 staining was present in 34% (37 of 109) of all sarcomas with most cases demonstrating weak (1+) staining. A few cases showed strong nuclear staining, such as low grade fibromyxoid sarcoma, synovial sarcoma, alveolar soft part sarcoma, and chondrosarcoma.

TUMOR TYPE	PAX8 Positive	Total cases	Percent (%)
Alveolar soft part sarcoma	3	3	100
Low grade fibromyxoid sarcoma	3	3	100
Malignant solitary fibrous tumor	3	3	100
Synovial sarcoma, monophasic type	5	6	83
Chondrosarcoma	6	10	60
Ewing/PNET	3	6	50
Carcinosarcoma (mesenchymal component)	3	6	50
Synovial sarcoma, biphasic type	1	2	50
Rhabdomyosarcoma	4	8	50
Osteosarcoma	3	9	33
Desmoplastic small round cell tumor	1	3	33
Leiomyosarcoma	2	16	13
Gastrointestinal stromal tumor	1	6	16
Adipocytic sarcomas	2	24	8
Extra skeletal chondromyxoid sarcoma	0	4	0
Endometrial stromal sarcoma	0	4	0
Adenosarcoma	0	1	0
Adult fibrosarcoma	0	5	0
Dermatofibrosarcoma protuberans	0	5	0
Intimal sarcoma	0	1	0
Epithelioid sarcoma	0	1	0
Clear cell sarcoma	0	1	0
Pleomorphic fibroblastic/myofibroblastic sarcoma	0	7	0

Conclusions: This is the first study demonstrating PAX8 immunoreactivity in malignant mesenchymal neoplasms. Although this expression is of unclear significance, and likely represents an aberrant immunohistochemical staining pattern (as these tissues do not relate to PAX8 embryologically), awareness of this finding is important in order to avoid diagnostic pitfall. We have demonstrated that PAX8 expression is not specific of epithelial neoplasms and, on the contrary, is positive in a significant subset of sarcomas.

91 Programmed Cell Death 1 (PD-1) Is Over Expressed in Giant Cell Tumor of the Bone and Adamantinoma

Alireza Torabi, Brad A Bryan, Clarissa N Amaya, Frank H Wians. Texas Tech University Health Science Center, El Paso, TX.

Background: PD-1 and its ligands have been shown to play a significant role in evasion of malignant tumor cells from immune system. Many epithelial and hematopoietic malignancies have been shown to over-express PD-L1. Hence, FDA approved anti-PD-1 inhibitors for treatment of non-small cell lung carcinoma and recently has expanded the use of immunotherapy for metastatic urothelial cell carcinoma and Hodgkin lymphoma. However, the data regarding expression of PD-1 and its ligands in bone and soft tissue malignancies are sparse. In this study, we evaluate the expression of PD-1 and PD-L1 in primary bone tumors, specifically giant cell tumor of the bone and adamantinoma.

Design: Tissue microarray (TMA) glass slide containing duplicate formalin fixed, paraffin embedded (FFPE) tissue specimens from giant cell tumor of bone (n=20) and adamantinoma (n=8) was obtained commercially. We performed IHC staining of the tissue sections for PD-1 receptor protein and its ligand (PD-L1) using an anti-PD-1 antibody (clone ab89828; Abcam, Cambridge, MA) and two anti PD-L1 antibodies (clone ab58810 and ab205921; Abcam, Cambridge, MA). Two individuals (AT and BB) examined the stained slide for the percentage of PD-1 and PD-L1 positive cells using the scores: 0, no staining (negative); 1, <50% of cells stained (weakly positive); and, 2, ≥50% of cells stained (positive). Normal bone tissue (n=9) was used as normal counterpart.

Results: Giant cell tumor of the bone and adamantinoma over-expressed PD-1 relative to normal bone tissue (p value <0.0001). PD-1 expression was detected in osteoclast-like giant cells as well as round/spindle mononuclear cells in the giant cell tumor and both epithelial and osteofibrous components of adamantinoma. PD-L1 was completely negative in these two primary tumors of the bone.

Conclusions: Our results showed over-expression of PD-1 in giant cell tumor of the bone and adamantinoma, while PD-L1 was negative. These two tumors can be locally aggressive and recur if not resected completely. Rarely, metastasis to the lung or other organs can happen. The data we discovered would raise the possibility of immunotherapy in the management of primary tumors of the bone.

92 Primary Breast Sarcomas : Clinico-Pathological Study of 16 Cases

Jen-Wei Tsai, Lei Huo, Samia Khan, Khalida Wani, Alexander J Lazar, Wei-Lien Wang. EDA Hospital, Kaohsiung, Taiwan; The University of Texas MD Anderson Cancer Center, Houston, TX.

Background: Non-radiation associated and non-vascular primary breast sarcomas are exceeding rare and account for less than 0.1% of breast malignancies. The diagnosis of primary breast sarcoma is challenging and is often one of exclusion because of its mimics, such as metaplastic carcinoma and malignant phylloides tumors. We examined primary breast sarcomas, which were not radiation associated or vascular in origin, at a single institution.

Design: The pathology database from The University of Texas MD Anderson cancer was examined from 2000 to 2016. Radiation induced sarcomas, metastatic sarcoma, those arising in chest wall bone and soft tissue sarcomas were excluded. Cases with any keratin staining, vascular differentiation and any suggestion of a biphasic breast tumor were excluded. Pathology slides were reviewed and clinical history and follow up was obtained.

Results: Sixteen tumors met our selection criteria. All were female patients aged from 34 to 72 years (mean, 49 years). 10 tumors arose from left breast, 6 from right breast. The operation method included mastectomy (n=14) and lumpectomy (n=2). The tumors ranged from 2.8 to 35 cm in greatest dimension (mean, 9 cm). The majority were high-grade undifferentiated pleomorphic or spindle cell sarcoma; one low-grade unclassified lipomatous tumor was encountered. Mean mitotic rate was 22 mitoses/10 hpfs. Mean tumor necrosis was 20%. One case of pleomorphic sarcoma occurred in the setting of a breast implant. 10 patients were treated by combination chemo- and radiotherapy, 2 by radiotherapy alone, and 2 by chemotherapy alone. Three patients had local recurrence; 7 patients developed distant metastasis (to lung and/or bone); median time to metastases was 8.1 months. Mean follow-up was 31.6 mos (range, 5 to 107); 5 died of disease, 1 alive with disease, 10 alive without disease.

Conclusions: Primary breast sarcomas are very rare. Most showed features of undifferentiated pleomorphic sarcomas, are high-grade and with poor prognosis and strong propensity for distant metastases. Molecular studies to further understand the relationship of these tumors to other sarcomatoid tumors in the breast are on-going.

93 Telomerase Maintenance Mechanism in Chordomas

Jen-Wei Tsai, Alan Meeker, Hong Cheuk Leung, Heather Lin, Davis R Ingram, Samia Khan, Khalida Wani, Laurence D Rhines, Alexander J Lazar, Wei-Lien Wang. EDA Hospital, Kaohsiung, Taiwan; The University of Texas MD Anderson Cancer Center, Houston, TX; John Hopkins School of Medicine, Baltimore, MD.

Background: Chordomas are rare malignant tumors with notochordal differentiation involving the axial skeleton. These tumors are locally aggressive and respond poorly to chemo- and radiotherapy. Although multiple molecular pathways in chordoma tumorigenesis have been investigated for targeted therapy, reliable prognostic biomarkers are lacking. Recently, alternative lengthening of telomere (ALT) has been demonstrated in 10%-15% of cancers, especially frequent in sarcomas with complex genetic karyotype. This pathway counteracts senescence and apoptosis. We investigated telomere maintenance mechanism in a large cohort of chordomas.

Design: Axial skeleton chordomas (n=93) were retrieved and a tissue microarray was constructed. The expression of ATRX and DAXX was investigated in tumor cells by immunohistochemistry. Alternative lengthening of telomeres was assessed by telomere-specific fluorescence in-situ hybridization (FISH), while telomerase gene promoter mutations were assessed by PCR and Sanger sequencing. Clinico-pathological parameters were tabulated from electronic medical records.

Results: ATRX nuclear expression was lost in 24 cases (31%, 24/77, ≤5% nuclear staining), DAXX expression lost in 14 cases (19%, 14/73, ≤5% nuclear staining). Alternative lengthening of telomere phenotype was identified in 38 cases (57%, 38/67). Telomerase (*TERT*) promoter mutation analysis demonstrated mutation (C228T) in only 7 cases (9%, 7/82), while 91% (75/82 cases) lacked mutation. Among the 7 tumors with TERT promoter mutation, 4 tumors were also ALT positive. Patients with ATRX loss had inferior overall survival (p=0.0423) and inferior progression free survival (p=0.0252). **Conclusions:** ATRX loss in chordoma was associated with more aggressive disease course. A significant portion of chordomas utilize ALT as a telomerase maintenance mechanism, suggesting that ATR inhibitors could be considered as treatment.

94 Immune Microenvironment in Chordomas

Jen-Wei Tsai, Cheuk Hong Leung, Heather Lin, Davis R Ingram, Khalida Wani, Laurence D Rhines, Alexander J Lazar, Wei-Lien Wang. EDA Hospital, Kaohsiung, Taiwan; The University of Texas MD Anderson Cancer Center, Houston, TX.

Background: Immunotherapy is an emerging treatment modality being explored for in many cancers, including sarcomas. However, little is known about the immune microenvironment in chordomas, which often have a lymphocytic infiltrate. This study examines the status of immune infiltrates in chordomas and correlates them with other molecular biomarkers, clinico-pathological features, and evaluates their prognostic significance.

Design: 93 cases of axial skeleton chordoma were retrieved and a tissue microarray was constructed. The immune infiltrates (CD3+, CD4+, CD8+, CD163+) in tumors were highlighted by immunohistochemistry and analyzed for density using image analysis. PRAME, a tumor associated antigen and PD-L1 (Dako clone 22C3) expression was examined by immunohistochemistry in tumor cells. Clinico-pathological parameters were tabulated from electronic medical records.

Results: The density of immune infiltrate is as follows: CD3+ intratumoral T lymphocyte (0 to 1121/mm²; median, 40.2); CD3+ stromal T lymphocyte (0 to 4339/mm²; median 560.3); CD4+ intratumoral T lymphocyte (0 to 751.1/mm², median 3.6); CD4+ stromal T lymphocyte (0 to 1460/mm²; median 44.3); CD8+ intratumoral T lymphocyte (0 to 498.1/mm²; median 8.2); CD8+ stromal T lymphocyte (0 to 1356/mm²; median 50); CD163+ intratumoral macrophages (0 to 2515/mm²; median 139.6); CD163+ stromal macrophages (0 to 5803/mm²; median 673.5). Despite the lymphocytic infiltrates, all tumors were negative for PD-L1, except one with weakly positive membrane staining. No PD-L1 positive immune cells are identified. Primary specimen had higher intratumoral density of CD4+ lymphocytes than recurrent and metastatic specimens (p=0.0368). PRAME expression was correlated with intratumoral density of CD3+ lymphocytes (p=0.0105). Age at diagnosis was correlated with CD163+ macrophage density in stroma (p=0.0444). No association with survival was seen with immune infiltrates (CD3+, CD4+, CD8+, CD163+).

Conclusions: Although there are inflammatory infiltrates in chordomas, their presence did not predict clinical outcome. PD-L1 was not expressed in either tumor cells or inflammatory cells, suggesting a different mechanism suppressing the immune surveillance. Further studies of the prognostic implications of immune infiltrates in chordoma are warranted.

95 PAX8 Expression by Solitary Fibrous Tumor: A Diagnostic Pitfall

David Ullman, Tiffany Graham, Shi Wei, Jennifer Gordetsky, Todd Stevens. University of Alabama at Birmingham, Birmingham, AL.

Background: Expression of PAX8, a member of the paired box family of genes, is typically limited to tumors of Mullerian, renal & thyroid origin but may rarely be seen in epithelial tumors of other primaries. PAX8 may be used as a diagnostic aid in retroperitoneal (RP) spindle cell tumors & one would assume that PAX8 positivity in a spindled RP tumor would be diagnostic of sarcomatoid renal cell carcinoma (SRCC). However, PAX8 expression in solitary fibrous tumor (SFT), a tumor not uncommon to the RP, has not been extensively studied. We investigated the expression of PAX8 in SFTs and other spindle cell tumors that can be found in the retroperitoneum.

Design: A retrospective review of our surgical pathology database was performed. We identified 31 SFT, 23 clear cell RCCs with sarcomatoid features, 3 gastrointestinal stromal tumors, 2 molecularly confirmed synovial sarcomas, 1 dedifferentiated liposarcoma of RP & 1 sclerosing liposarcoma of RP. All were stained with PAX8 (Biocare, rabbit polyclonal, 1:50) & STAT6 (Abcam, rabbit monoclonal, clone YE361, 1:200) on a DAKO autostainer. Diffuse expression of PAX8 was defined as ≥30% expression in tumor cells. Chi-square statistical analysis was performed.

Results: Of the 31 SFTs, 14 were pleural based, 17 extrapleural, and 8 were histologically malignant. 13/31 (42%) and 29/31 (94%) SFTs showed nuclear expression of PAX8 and STAT6, respectively. Of the 13 SFT showing PAX8 expression, 8 showed diffuse PAX8 expression (>90% of tumor in 5, 50% in 2 & 30% in 1) & 5 expressed PAX8 focally (5-15% of tumor in 4 cases and 1 tumor with 1%). A significantly higher proportion of extrapleural SFTs expressed PAX8 compared to pleural SFTs (59% vs. 21%; p=0.0357). 3/8 (38%) histologically malignant SFTs showed PAX8 expression (diffuse & strong in 2, focally in 1) while 10/23 (43%) histologically benign SFT expressed PAX8 (p=0.768). 20/23 (87%) SRCC expressed PAX8; the sarcomatoid component of all 23 SRCC was negative for STAT6, however in 1 case the conventional clear cell component only showed focal (1%) weak STAT6 expression. Of the other spindle cell tumors studied, PAX8 expression was only seen in the sclerosing liposarcoma (diffuse expression) and in 1 synovial sarcoma (50% of tumor cells; tricep primary).

Conclusions: Pathologists should be aware of the potential pitfall of the relatively frequent expression of PAX8 by SFT. Extrapleural SFTs were statistically more likely to express PAX8 than pleural SFT. PAX8 expression by a spindle cell lesion of retroperitoneum would not allow distinction between SFT, SRCC, or sclerosing liposarcoma. A STAT6+/PAX8+ phenotype excludes SRCC.

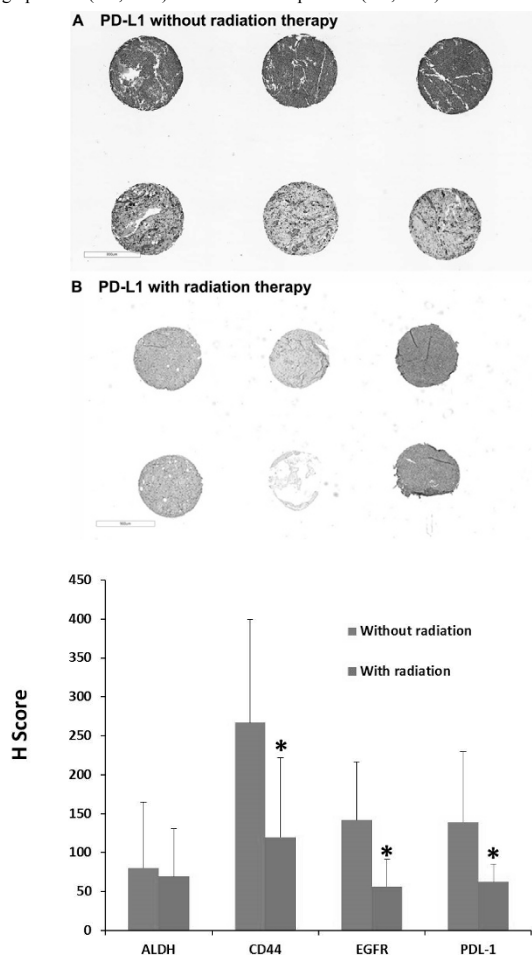
96 Radiation Therapy Related Down-Regulation of PD-L1 on High-Grade Poorly Differentiated Sarcomas Justify the Combined Radio-Immunotherapy

Dongguang Wei, Robert J Canter, Hong Qiu, Arta M Monjazeb, Mingyi Chen. UC, Davis, Sacramento, CA.

Background: Successful multimodality management of advanced soft tissue sarcomas (STS) remains a clinical challenge. Although immune checkpoint blockade has shown great promise, only a minority of patients respond. Improved biomarkers could benefit the treatment choice, since cytotoxic therapies and radiotherapy (RT) can alter the immune milieu. The objective of this study was to characterize PD-L1 expression in locally advanced STS with or without preoperative RT.

Design: Tissue microarrays (TMA) were constructed using formalin-fixed, paraffin-embedded STS cases (N=17). A composite H-scoring system was applied to analyze/quantify the protein expression. TMA sections were immunostained using a rabbit anti-human PD-L1 antibody (Sino Biological, Clone: 015). The intensity and percentage of PDL-1-positive cells were calculated and scored blindly. Patients were categorized into PD-L1 high and low-expressing based on H-score above or below the median. Parametric and non-parametric statistics were used as appropriate.

Results: Mean age was 55±21, 82% were female, and 53% of STS tumors were located on the extremity. Median tumor size was 15.5 cm (range 2.4-24.8 cm). Half of the cases received preoperative RT. We observed 9 recurrences, and 5 sarcoma deaths. Overall, PD-L1 expression was significantly lower among RT patients (62.5±23.1 vs 139±90.5, p=0.04), and tumor stem cell markers EGFR/CD44 were also significantly lower among chemotherapy patients (p < 0.05). Distant recurrences were more common in PDL-1 high patients (5/8, 62%) than PDL-1 low patients (2/9, 22%).



Conclusions: RT is associated with decreased PD-L1 expression in locally advanced STS, and lower PD-L1 expression is associated with improved long-term outcome. The modulation of PDL-1 expression by RT and the impact on prognosis in STS warrants further study.

97 Clinicopathological and Molecular Features of Dedifferentiated Liposarcoma with Ossification: A Comparative Study with Dedifferentiated Liposarcoma without Ossification and Extraskeletal Osteosarcoma

Kyoko Yamashita, Kenichi Kohashi, Yuichi Yamada, Yoshinao Oda, Shinya Toyokuni. Nagoya University Graduate School of Medicine, Nagoya, Japan; Graduate School of Medical Sciences, Kyushu University, Fukuoka, Japan.

Background: Dedifferentiated liposarcoma (DDLPS) sometimes exhibit heterologous differentiation, and its influence on prognostic outcome is still controversial. As for ossification, it is also not clear whether the bone component means heterologous differentiation or it can be formed by reactive (non-neoplastic) mesenchymal cells. We aimed to investigate the neoplastic nature of the bones formed in DDLPS, and make clear the clinical and pathological characteristics of DDLPS with ossification.

Design: We examined 27 cases of DDLPS with ossification by comparing them with 24 cases of DDLPS without ossification and 17 cases of primary extraskeletal osteosarcoma (ESOS) without MDM2 amplification or overexpression. The clinical and pathological findings were reviewed. Histological grade was determined using 'modified' FNCLCC grading system proposed before emphasizing the importance of tumor differentiation scoring.

Results: MDM2 amplification was confirmed in osteocytes and/or osteoblastic cells in all DDLPS cases with ossification where Fluorescence In-Situ Hybridization (FISH) was successfully performed in bone forming area (22/22). The bones found in DDLPS were mainly mature in most cases (20/27), and some of them could be described as "metaplastic." The bones were often predominantly formed in the peripheral part of the dedifferentiated area, which means close to well-differentiated liposarcoma area (14/27). Although some DDLPS cases had relatively high grade area with immature bone formation similar to conventional osteosarcoma (4/27), immature lace-like osteoid formation among highly atypical cells arranged in high density, which was often seen in ESOS (7/17), was not observed in DDLPS. Histologically, DDLPS with ossification tends to be lower grade than DDLPS without ossification, while ESOS showed highest grade (mean grade: 1.85 vs 2.10 vs 2.41). The clinical outcome, such as overall survival, of DDLPS with ossification was at least not worse than DDLPS without ossification although significant difference could not be identified.

Conclusions: The bones formed in DDLPS cases were confirmed to be neoplastic regardless of their morphology and maturity, which means osteogenic differentiation of tumor cells. We found osteogenic differentiation of DDLPS could be associated with lower histological grade, and possibly better prognosis.

98 Clinicopathological and Molecular Characterization of SMARCA4-Deficient Thoracic Sarcomas with Comparisons to Potentially Related Disease Entities

Akihiko Yoshida, Eisuke Kobayashi, Takashi Kubo, Toru Motoi, Noriko Motoi, Akira Kawai, Takashi Kohno, Hiroshi Kishimoto, Hitoshi Ichikawa, Nobuyoshi Hiraoka. National Cancer Center, Tokyo, Japan; Komagome Hospital, Tokyo, Japan; Saitama Prefectural Children's Hospital, Saitama, Japan.

Background: A growing number of studies have suggested critical tumor suppressor roles of the SWI/SNF chromatin remodeling complex in human cancers. The recent discovery of SMARCA4-deficient thoracic sarcomas (SMARCA4-DTS, Le Loarer et al. Nat Genet, 2015) has added to the list of tumor groups with the SMARCA4 inactivating mutation.

Design: To better characterize these tumors and establish their nosological status, we undertook a clinicopathologic and molecular analysis of 12 SMARCA4-DTSs and compared them with malignant rhabdoid tumors (MRTs), epithelioid sarcomas (ESs), and SMARCA4-deficient lung carcinomas (SMARCA4-DLCs).

Results: Eleven men and one woman with SMARCA4-DTS (aged 27-82 years, median 39 years) were included in the study. Most of the patients had heavy smoking exposure and pulmonary emphysema/bullae. The primary tumors were large and involved thoracic region in all cases, and simultaneously affected abdominal cavities in 3 cases. The patients followed a rapid course, with a median survival of 7 months. Histologically, all tumors showed diffuse sheets of mildly discohesive, relatively monotonous, undifferentiated epithelioid cells with prominent nucleoli. Immunohistochemically, all tumors demonstrated a complete absence (8 cases) or diffuse severe reduction (4 cases) of SMARCA4 expression. Cytokeratin, CD34, SOX2, SALL4, and p53 were expressed in 50%, 83%, 83%, 83%, and 70% of cases, respectively. SMARCA2 expression was deficient in 92% of cases. The targeted sequencing was successful in 5 cases and demonstrated the inactivating SMARCA4 mutation in each case (including that with reduced SMARCA4 expression), and additionally uncovered alterations in TP53 (5/5), NF1 (2/5), CDKN2A (2/5), KRAS (1/5), and KEAP1 (1/5), among others. In a comparative analysis, aside from clinical and some morphological differences, immunohistochemical profiles were found different among entities: 13 MRTs expressed CD34 in 46%, SOX2 in 77%, SALL4 in 92%, and p53 in 0% of cases, while they lacked SMARCB1 in 85%, SMARCA4 in 15%, and SMARCA2 in 50% of cases; 15 ESs expressed CD34 in 73%, SOX2 in 7%, and SALL4 in 7% of cases, while they lacked SMARCB1 in 100% and SMARCA2 in 13% of cases; 12 SMARCA4-DLCs expressed CD34 in 0%, SOX2 in 33%, and SALL4 in 0% of cases, while they lacked SMARCA4 in 100% and SMARCA2 in 8% of cases.

Conclusions: SMARCA4-deficient thoracic sarcomas constitute a unique entity that requires recognition and differentiation from other epithelioid malignancies in adults.

Breast Pathology

99 Expression of Met and Androgen Receptors in ER Negative Breast Cancer

Dalia Abouelfadl, Hebatallah A Amin, Noha N Yassen, Marwa E Shabana, Heba A Abdelal. National Research Center, Cairo, Egypt; Egyptian Forensic Authority, Cairo, Egypt; Armed Forces Hospitals, Cairo, Egypt.

Background: Human breast cancers are heterogeneous. This heterogeneity may originate due to differences in the target cell population and/or it may be the result of different combinations of mutations in a normal breast progenitor cell. New therapeutic targets are needed in breast cancer, particularly in patients with TNBC and the related basal-like subgroup. The Met tyrosine kinase receptor activates cell proliferation and a strong relationship between high HGF/Met signaling and tumor progression was found. The biologic roles of Androgen receptors in the breast are incompletely understood since it is unclear whether the effects of androgens on breast cells are predominantly proliferative or anti-proliferative. The purpose of this study is to determine the prognostic value of Met and AR expression in ER negative breast cancer patients that might be useful information to treat breast cancer especially TNBC.